Ensuring Advancement in Sandwich Construction Through Innovation and Exploitation

REPORT

No.: D3.3 – part 1

Stabilisation of beams by sandwich panels

Publisher: Saskia Käpplein
Thomas Misiek
Karlsruhe Institute of Technology (KIT)
Versuchsanstalt für Stahl, Holz und Steine

Task: 3.2
Object: Stabilisation of beams by torsional restraint

This report includes 61 pages and 3 appendices.

Date of issue: 17.05.2011

Versuchsanstalt für Stahl, Holz und Steine, Karlsruhe Institute of Technology (KIT) Tel.: +49 (0)721 608 42215
Abt. Stahl- und Leichtmetallbau, 76128 Karlsruhe, Deutschland Fax: +49 (0)721 608 44078

Project co-funded under the European Commission Seventh Research and Technology Development Framework Programme (2007-2013) Theme 4 NMP-Nanotechnologies, Materials and new Production Technologies		
Prepared by		
Saskia Käpplein, Thomas Misiek, Karlsruhe Institute of Technology (KIT), Versuchsanstalt für Stahl, Holz und Steine		
Drafting History		
Draft Version 1.1	10.05.2011	
Draft Version 1.2		
Draft Version 1.3		
Draft Version 1.4		
Final	17.05.2011	
Dissemination Level		
PU	Public	X
PP	Restricted to the other programme participants (including the Commission Services)	
RE	Restricted to a group specified by the Consortium (including the Commission Services)	
CO	Confidential, only for members of the Consortium (including the Commission Services)	
Verification and approval		
Coordinator		
Industrial Project Leader		
Management Committee		
Industrial Committee		
Deliverable		
D3.3 – part 1: Stabilisation of beams by sandwich panels		Due date: Month 35 Completed: Month 32

Table of contents

1 Preliminary remarks

Sandwich panels increase the resistance of substructures (beams, purlins) against lateral torsional buckling by restraining the rotations and lateral displacements.

The torsional restraint is governed by the stiffness of the connection of the sandwich panel to the substructure. Recent research carried out at UKA showed that this stiffness significantly depends on the lateral load transferred by the sandwich panel. Formulae for calculating the parameters of this moment-rotation-relation are given for sandwich panels with two different core materials. So far only connections through the lower crimp with two fasteners per element have been investigated. Other types of connections (e.g. connection through upper crimp with calottes) and different core materials are important yet unknown parameters of the moment-rotation-relation.

A design concept for the quantification and calculation of the stabilising effects on beams under predominantly static loading by sandwich panels was developed within the framework of the EASIE project. This will be introduced in this report. We will start with a presentation of the start of the art.

The investigations will then start with some general considerations regarding the basic mechanical model. The influence of the different parameters of the mechanical model will be studied in a parametrical study. Finally, the tests at hand will be evaluated on the basis of the mechanical model.

2 State of the art

Different to profiled sheeting, publications on the rotational restraint of beams provided by sandwich panels are rather rare.

In [1] and [2] experimental investigations on the torsional restraint of thin-walled Z-sections are presented.

[1] gives some results of numerical investigations. The publication ends up with the linear design formula for the rotational stiffness

$$c_{\vartheta} = k \cdot b_K^2 \qquad \textbf{(1)}$$

with the spring stiffness k and lever arm b_K between the fastener and the line of contact. No values for the actual spring stiffness of k are given; therefore the application of the results is not possible. The investigations [2] lead to formula of the form

$$c_\vartheta = \alpha_1 \cdot E_C \cdot t_K^2 \cdot \left(\frac{f_y}{E}\right)^{\alpha_2} \cdot \left(\frac{f_t}{h_s}\right)^{\alpha_3} \cdot \left(\frac{f_l}{f_\beta}\right)^{\alpha_4} \cdot \left(\frac{b_K}{b_w}\right)^{\alpha_5} \quad \textbf{(2)}$$

with f_t, h_s, f_l, f_β and b_w being dimensions of the outer face.

Both investigations neglect the effects of the loading by using the test set-up introduced in N 1993-1-3, Annex A.5. This test set-up, called the Peköz test, was originally developed for unsymmetric thin-walled purlins such as Z-sections. During the tests, no loading is applied. The effect of the direction of loading is incorporated by simply rotating the purlin in different directions. While this test set-up is rather questionable for profiled sheeting, it is even completely bogus to apply with sandwich panels because of the influence of indentation of the beam and/or the fastener into the panel. Compared to this, the distortion of the beam can be neglected. Consequently, [2] states that “the impact of uplift and gravity loading is not straightforward”, which is true when incorporating the direction of loading only by the direction of rotation. The investigations presented in [1] showed the same missing tendency. As a further result of this negligence of the loading, the formulae presented in [1] and [2] both assume a linear model for the rotational stiffness.

In [3] an extensive investigation of the rotational restraint of beams provided by the panels is presented. The results of these experimental und numerical investigations leaded to a design concept and design formulae ready to be incorporated into a design code. The concept was validated for hot-rolled sections but also C- and Z-sections. [3] gives a bilinear moment-rotation curve with

$$c_{\vartheta 1} = c_1 \cdot E_C \cdot \frac{b}{82} \quad \textbf{(3)}$$

and

$$c_{\vartheta 2} = c_2 \cdot E_C \cdot t_K \cdot \frac{b}{82} \quad \textbf{(4)}$$

A linear dependency on the width b is assumed.

Most recently, the German design code for steel structures, DIN 18800-2, was updated, now including the possibility to use sandwich panels for the stabilisation of beams against lateral-torsional buckling. These regulations are based on the investigations described in [3]. They are shown in the following tables. The values of E_C, b and t_K have to be inserted with the units given in Tab. 1. The calculated values of $c_{\vartheta 1}$ and $c_{\vartheta 2}$ have the unit kN or kNm/m

	Double-symmetric beams with 60 mm ≤ b ≤ 100 mm	Z- or C-section 60 mm ≤ b ≤ 80 mm
$c_{\vartheta 1}$	$c_1 \cdot E_C \cdot \frac{b}{82}$	$c_1 \cdot E_C$
$c_{\vartheta 2}$	$\zeta \cdot c_2 \cdot E_C \cdot t_K \cdot \frac{b}{82}$	0
m_k	$q_d \cdot \frac{b}{82}$	$q_d \cdot b$

2,0 N/mm² ≤ E_C ≤ 6,0 N/mm²	elastic modulus of the core layer
0,42 mm ≤ t_K ≤ 0,67 mm	sheet thickness of the outer face layer
b [mm]	width of the flange of the beam
q_d	design value of the downward load to be transferred from the panel to the beam
c_1, c_2	parameter according to Tab. 2
ζ	parameter depending on the pattern of fixings
	ζ = 1,0 alternating application of fixings
	ζ = 1,5 one-sided application of fixings
	ζ = 0,0 hidden fixings

Tab. 1: Rotational stiffness $c_{\vartheta 1}$ and $c_{\vartheta 2}$

Core material	Application	Geometry of outer face layer (at the head of the fasteners)	c_1	c_2
PUR	roof	profiled	1,44	0,22
	wall	lightly profiled/flat	1,20	0,38
Mineral wool	roof	profiled	0,69	0,18
	wall	lightly profiled/flat	0,48	0,16

Tab. 2: Parameters c_1 and c_2

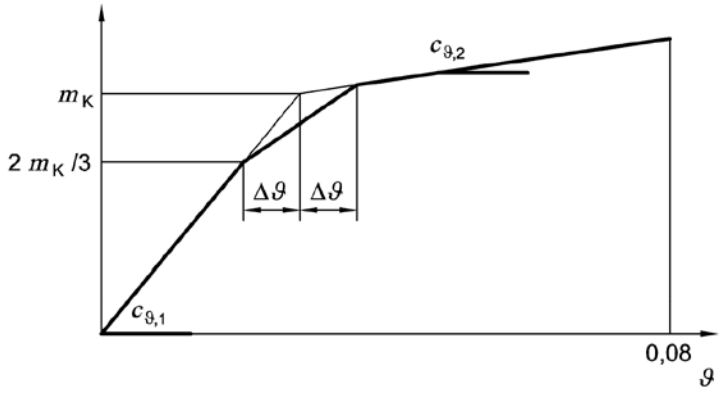

Fig. 1: Moment–rotation-relation

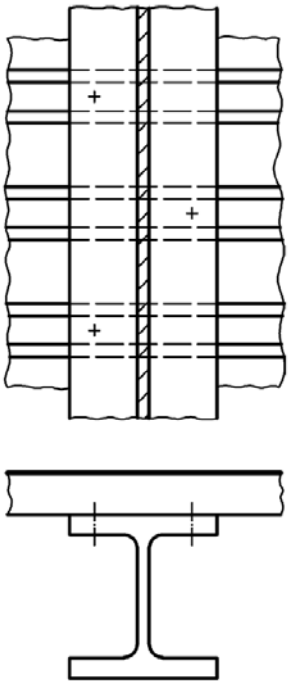

alternating application of fixings

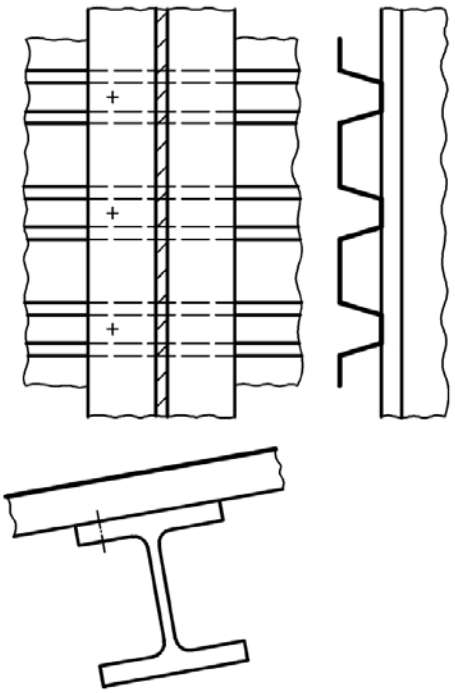

one-sided application of fixings,

Fig. 2: Fixing patterns

The basic construction of the formulas (derivation of the influencing parameters) for $c_{\vartheta 1}$ and $c_{\vartheta 2}$ was derived from an FE-analysis whereas the parameters c_1 and c_2 were derived from a statistical evaluation of test results,

The regulations are restricted to downward loading and to the core materials PUR and mineral wool. Also, the parameter range for E_C and t_K is restricted.

The underlying investigations [3] also cover aspects of serviceability. It was found that water tightness was given for rotations up to ϑ = 0,08. With this value, also local plastic deformations of the faces did not occur.

3 Theoretical considerations on c_ϑ

3.1 Introduction

The following considerations focus on simple mechanical models for understanding the basic behaviour in the connection between the flange of the beam and the sandwich panel. For better understanding, the general description of the effects under deadweight loading is given here. This description is based on [4].

3.2 General description of the effects under deadweight loading

Fig. 3 shows a generalised moment-rotation-relation for the spring stiffness of the connection of a sandwich panel under deadweight loading.

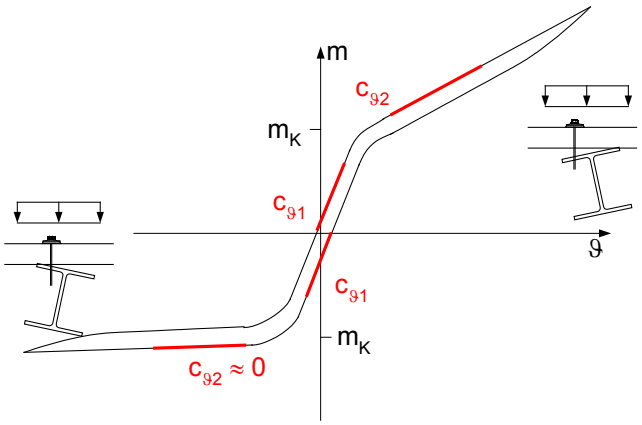

Fig. 3: Generalised moment-rotation-relation for deadweight loading

In this generalised relation we assume that all of the fasteners are mounted on one side of the web as shown in Fig. 3. Here, the positive direction of rotation is defined as an anticlockwise rotation.

We can differentiate three parts of the moment-rotation-relation. For small rotations ϑ, there is the value $c_{\vartheta 1}$. The load q acting on the panel is always transferred by contact from the inner face of the panel to the upper flange of the beam. The rotational stiffness only depends on the width of the flange and the indentation stiffness (Fig. 4). This indentation stiffness is dominated by the compression stiffness E_{Cc} of the core material. The rotational stiffness does not depend on the position of the fasteners because the fasteners are not activated in this situation.

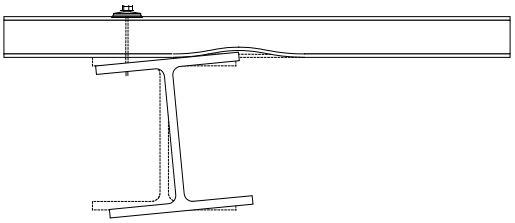

Fig. 4: Mechanical model for $c_{\vartheta 1}$

The area of contact decreases, with increasing rotation until it is reduced to the final contact line with the outer edge of the flange. At this stage, the restoring moment is the contact moment

$$m_K = \frac{q \cdot b}{2} \qquad \textbf{(5)}$$

When the deflecting moment to be stabilized exceeds the contact moment m_K the value $c_{\vartheta 2}$ applies. At this stage, tensile forces in the fasteners are activated. These tensile forces F_t cause an indentation u_w of the fasteners' heads and washers into the outer face of the sandwich panel. This additional deformation decreases the stiffness significantly: The value $c_{\vartheta 2}$ is significantly smaller than the value $c_{\vartheta 1}$.

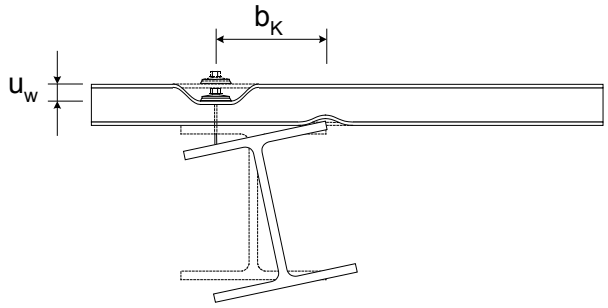

Fig. 5: Mechanical model for $c_{\vartheta 2}$ – positive rotations ϑ

The value $c_{\vartheta 2}$ depends on the indentation stiffness $K_{\vartheta 2}$ of the fastener and the indentation stiffness $k_{\vartheta 1}$ at the line of contact at the outer edge of the flange. This stiffness depends on the direction of rotation as defined in Fig. 3 with regard to the position of the fastener and the distance b_K of the fastener from the contact line as defined in Fig. 5. For positive rotations we still have a distinct value of $c_{\vartheta 2}$, while for negative rotations $c_{\vartheta 2}$ is comparatively small because of the small distance b_K and the small corresponding contribution to the restoring moment. With an alternating fixing pattern the values $c_{\vartheta 2}$ are the same for both directions of rotation, provided b_K is the same for both directions of rotation. However, due to the aforementioned influence of the indentation stiffness of the fasteners head, the total number of fasteners has to be doubled. If not, the value $c_{\vartheta 2}$ reduces to half of the value.
Based on these general considerations, simplified mechanical models can be established.

3.3 Simplified mechanical model for $c_{\vartheta 1}$

The value $c_{\vartheta 1}$ can be derived by using a simplified mechanical model for the indentation stiffness of the core. Tensile forces in the fastener are not taken into account. Fig. 6 shows the model for the local indentation at the outer edge of the flange. Only one half of the flange is considered. It is assumed, that the point of indentation is exactly defined and the forces are only transferred at the tip of the outer edge of the flange. This is in fact not true for real behaviour. The indentation will lead to an area of contact with a resulting force with a lever arm smaller than b. This effect will be neglected in a first step.

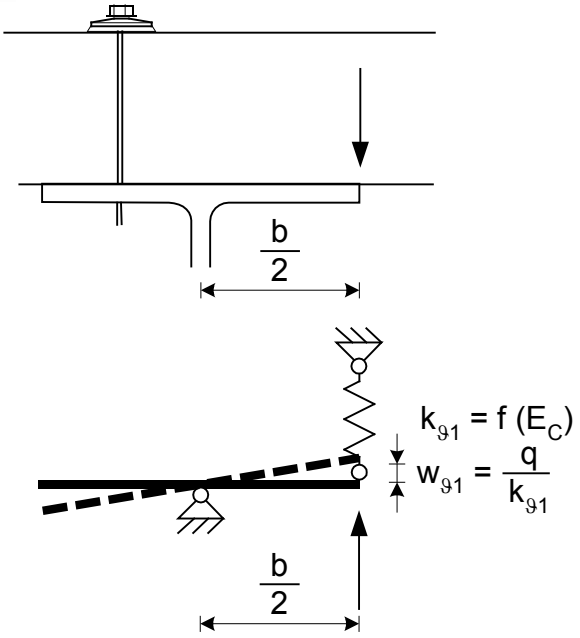

Fig. 6: Mechanical Model for the derivation of $c_{\vartheta 1}$

$$k_{\vartheta 1} = \frac{q}{w_{\vartheta 1}} = \frac{8 \cdot (1 - \nu_C)}{3 \cdot (1 + \nu_C) \cdot (3 - 4 \cdot \nu_C)} \cdot E_C \qquad \textbf{(6)}$$

Converted into the rotational spring stiffness, we have

$$c_{\vartheta 1} = \frac{m}{\vartheta} = \frac{q \cdot \frac{b}{2}}{2 \cdot \frac{w_{\vartheta 1}}{b}} = \frac{q \cdot b^2}{4 \cdot w_{\vartheta 1}} \qquad \textbf{(7)}$$

Based on the theory of a beam on an elastic foundation (Fig. 7), the relation between indentation and

$$w = \frac{q \cdot \lambda}{2 \cdot k} \cdot e^{-\lambda \cdot x} \cdot (\sin(\lambda \cdot x) + \cos(\lambda \cdot x)) \qquad \textbf{(8)}$$

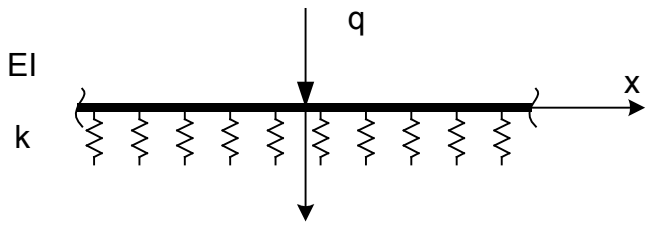

Fig. 7: Infinite beam on elastic foundation with spring stiffness k

with the characteristic

$$\lambda = \sqrt[4]{\frac{k}{4 \cdot E_F \cdot I_F}} \tag{9}$$

being of the order of "length^{-1}". The deflection w_0 under the load q at x = 0 is

$$w_0 = \frac{q \cdot \lambda}{2 \cdot k} \tag{10}$$

From the theory of buckling of plates on elastic foundation, the relation

$$k = \frac{2 \cdot (1 - \nu_C)}{(1 + \nu_C) \cdot (3 - 4 \cdot \nu_C)} \cdot \pi \cdot \sqrt{\frac{1}{l_a^2} + \frac{1}{l_b^2}} \cdot E_C \tag{11}$$

between the spring stiffness and the elastic properties E_C and ν_C of the core material is known. The values l_a and l_b are the lengths of the sinusoidal half-wave. This relation is adopted for the beam problem, assuming $b \to \infty$ and a being the distance between the points of inflexion with the indentation w = 0. Thus,

$$l_a = \frac{3 \cdot \pi}{2 \cdot \lambda} \tag{12}$$

applies. Combining (11) and (12) with (10), we obtain

$$w_0 = w_{\vartheta 1} = \frac{q}{E_C} \cdot \frac{3 \cdot (1 + \nu_C) \cdot (3 - 4 \cdot \nu_C)}{8 \cdot (1 - \nu_C)} \cdot \tag{13}$$

or

$$k_{\vartheta 1} = \frac{q}{w_{\vartheta 1}} = \frac{8 \cdot (1 - \nu_C)}{3 \cdot (1 + \nu_C) \cdot (3 - 4 \cdot \nu_C)} \cdot E_C \tag{14}$$

Converted into the rotational spring stiffness, we have

$$c_{\vartheta 1} = \frac{m}{\vartheta} = \frac{q \cdot \frac{b}{2}}{2 \cdot \frac{w_{\vartheta 1}}{b}} = \frac{q \cdot b^2}{4 \cdot w_{\vartheta 1}} \tag{15}$$

and

$$c_{\vartheta 1} = \frac{2 \cdot (1 - \nu_C)}{3 \cdot (1 + \nu_C) \cdot (3 - 4 \cdot \nu_C)} \cdot b^2 \cdot E_C \tag{16}$$

Obviously, (16) does not incorporate all the stiffening effects which can be found in the test. For instance, (16) assumes an infinite half space, while in practice the outer face layer increases the spring stiffness of the elastic foundation $k_{\vartheta 1}$. Therefore roof panels have a higher rotational stiffness $c_{\vartheta 1}$ which might be also found with thicker wall panels. An adjustment based on test results is required, using the approach

$$c_{\vartheta 1} = c_1 \cdot E_C \cdot b^2 \qquad \textbf{(17)}$$

Nevertheless (16) gives a good approximation for stiff panels. The relation

$$c_{\vartheta 1}\left[\frac{kNm}{m}\right] = 1{,}60 \cdot \frac{b[mm]}{82mm} \cdot E_C\left[\frac{N}{mm^2}\right] \qquad \textbf{(18)}$$

was introduced in [1] for roof panels. This relation differs especially in the order of b, but with a flange width b = 82 mm for an IPE160 which used in the underlain tests, (16) gives

$$c_{\vartheta 1}\left[\frac{kNm}{m}\right] = 1{,}494 \cdot E_C\left[\frac{N}{m^2}\right] \qquad \textbf{(19)}$$

for ν_C = 0,0 or

$$c_{\vartheta 1}\left[\frac{kNm}{m}\right] = 1{,}344 \cdot E_C\left[\frac{N}{m^2}\right] \qquad \textbf{(20)}$$

for ν_C = 0,3 while (18) gives

$$c_{\vartheta 1} = 1{,}6 \cdot E_C \qquad \textbf{(21)}$$

for roof panels, all of them being in a close range. Fig. 8 shows a comparison of both formulae for ν_C = 0,3.

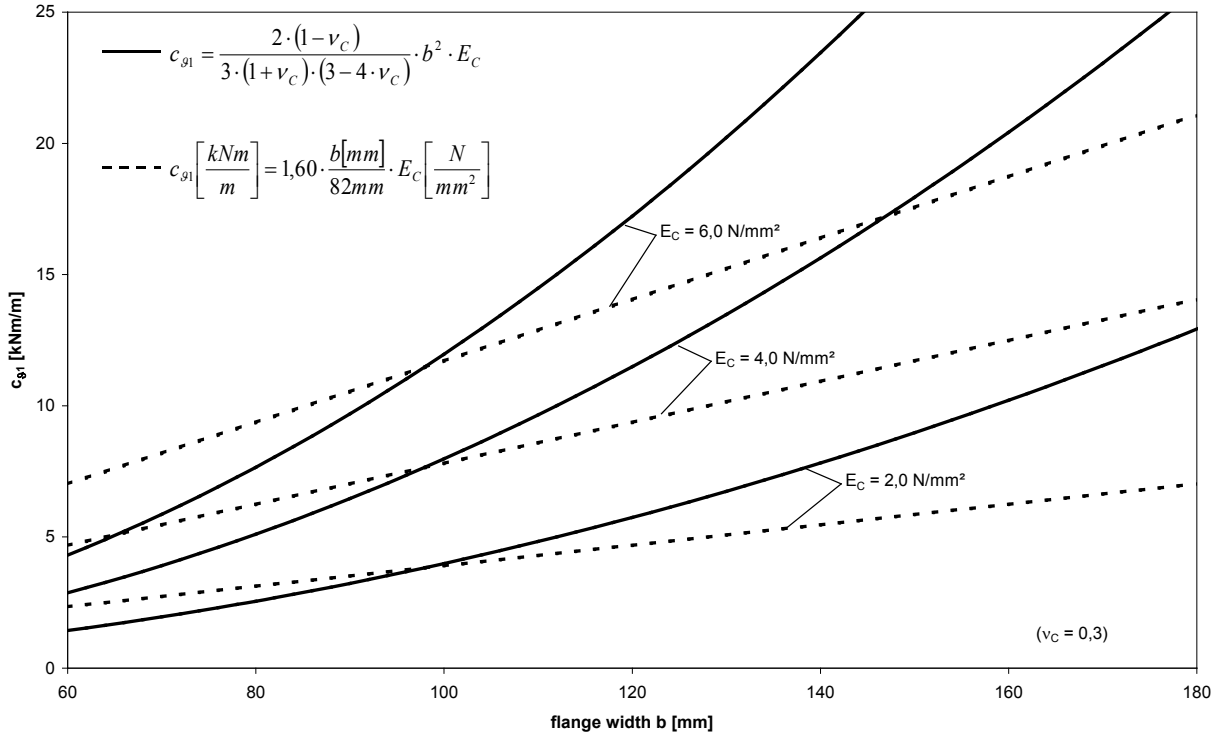

Fig. 8: Comparison between (16) and (18) for different values of E_C

Near the flange width tested in [1], the results of (18) are higher. In the parameter range of validity of b $\in$ [60; 80], a linear dependency is satisfying, but not explaining the difference in $c_{\vartheta 1}$. The derivation of the formula (18) is based on the evaluation of the test results.

3.4 Simplified mechanical model for $c_{\vartheta 2}$

The derivation of a simple mechanical model for c_{J2} is possible, too. The basic model is shown in Fig. 9.

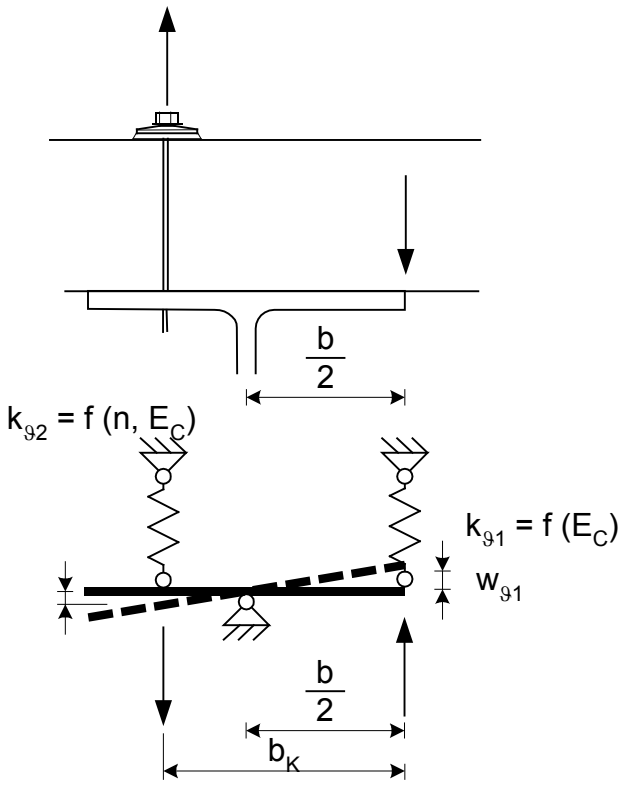

Fig. 9: Mechanical model for $c_{\vartheta 2}$

The model includes both the indentation of the flange and the indentation of the fastener:

$$\vartheta = \frac{|w_{\vartheta 1} + w_{\vartheta 1}|}{b_k} = \frac{\left|\frac{q_K}{k_{\vartheta 1}} + \frac{q_K}{n \cdot K_{\vartheta 2}}\right|}{b_k} \qquad \textbf{(22)}$$

Therefore the model consists of two springs. We obtain:

$$c_{\vartheta 2} = \frac{m}{\vartheta} = \frac{q_K \cdot b_K}{\frac{\left|\frac{q_K}{k_{\vartheta 1}} + \frac{q_K}{n \cdot K_{\vartheta 2}}\right|}{b_K}} = \frac{b_K^2}{\left|\frac{1}{k_{\vartheta 1}} + \frac{1}{n \cdot K_{\vartheta 2}}\right|} \qquad \textbf{(23)}$$

This it will be shown later this can be simplified to

$$c_{\vartheta 2} = n \cdot K_{\vartheta 2} \cdot b_K^2 \quad \textbf{(24)}$$

and finally

$$c_{\vartheta 2} = c_2 \cdot n \cdot E_C \cdot b_K^2 \quad \textbf{(25)}$$

4 Numerical investigations

4.1 Introduction

Numerical investigations were done to allow the study of the influence of different parameters on the torsional stiffness. These investigations were not used to determine the final values of stiffness but serve as a help to determine the relevant parameters. Theses parameters are:

- stiffness E_C of the core material
- stiffness E_F of the face material
- thickness t_a of the outer face
- thickness t_b of the inner face
- thickness D of the core
- width b of the flange of the beam
- depth of profiling
- type of loading

4.2 Description of the finite element model

For the numerical investigations on the stabilisation of beams the finite element model already used for the investigations described in [3] was used. Some supplementation had to be made to allow for the calculation of panels fixed in the upper flange or under uplift loading.
The finite element model covers the beam section, the stabilising sandwich panel as well as the fastener as detail of a roof or wall system with an infinite width. The longitudinal edges of the beam section as well as of the sandwich panels are provided with symmetric boundary conditions in such a way that a detail develops with a width of 1.0 m. Studies on the mesh convergence performed in advance, make sure that the finite element model supplies reliable results. Fig. 10 shows the schematic structure of the finite element model.

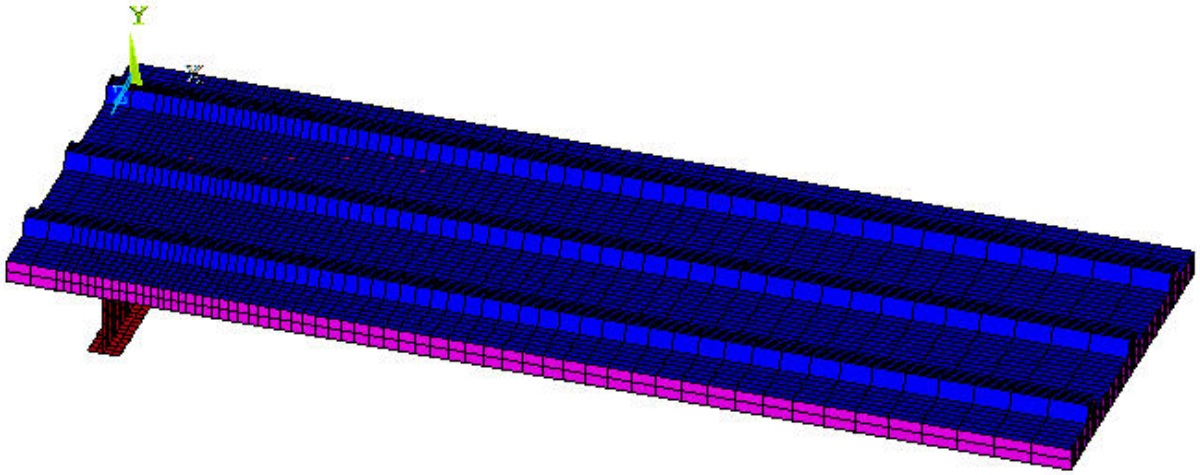

Fig. 10: Finite-Element-Model

The face layers of the sandwich panel, the sealing washer of the fastener as well as the beam section are modelled through shell elements of type SHELL181. This three-dimensional shell element has four corner joints with three degrees of freedom for displacement and three degrees of freedom for rotation. The element hast bending, membrane and shear stiffnesses and also includes non-linear material properties. For the face layers made of steel as well as for the beam section bi-linear constitutive equations (linear elastic, ideal plastic) were applied as material behaviour, where after exceeding the yield strength f_y yielding without strain hardening starts. For the face layers made of aluminium two different material laws were used, see chapter 4.3. For the face layers made of GFRP a linear elastic material model was used.

Modelling of the sandwich core layer is done through elements of type SOLID45, an isotropic, three-dimensional volume element with eight corner joints, having three degrees of freedom for displacement. Non-linear constitutive equations can also be considered with these elements. In the scope of the finite element modelling a homogenous and isotropic material is assumed, however, for reasons of simplification, unless otherwise expressly noted.

Fastening of the sandwich panel on the beam section is realised through elements of type LINK1. It concerns a two-dimensional element connecting two joints with each other for uniaxial transfer of both tension and compression forces. Both joints have two degrees of freedom for translation. A contact surface between the face layer and the upper flange of the beam sections serves for transferring the contact between the sandwich element and the beam section. This contact surface consists of contact elements of type CONTAC173 on the side of the sandwich panel and of contact elements type TARGET170 on the upper flange of the beam. Between these pairs of contact elements compression and shear forces can be transferred if the gap is closed. The contact elements have the same geometric properties as those elements that are connected to them.

The loadings in the finite element model are applied in two load steps corresponding to the loading sequence in the test. In the first step, three-dimensional loading of the face layer of the sandwich element is performed. As soon as the load level of the three-dimensional superimposed load is reached the second load step starts, in which the beam section is gradually distorted through moment acting in the rotation axis.

The evaluation of the finite element analysis is performed through reading the resulting beam rotation in dependence on the torsion moment applied gradually. The presentation is done as moment-torsion-relation corresponding to the experimental investigations, so that a comparison is directly possible.

Comparative calculations for the verification of the finite element model under downward loading are described in [3].

Fig. 11 and Fig. 12 show the local deformations during the different stages of the moment-rotation-relation.

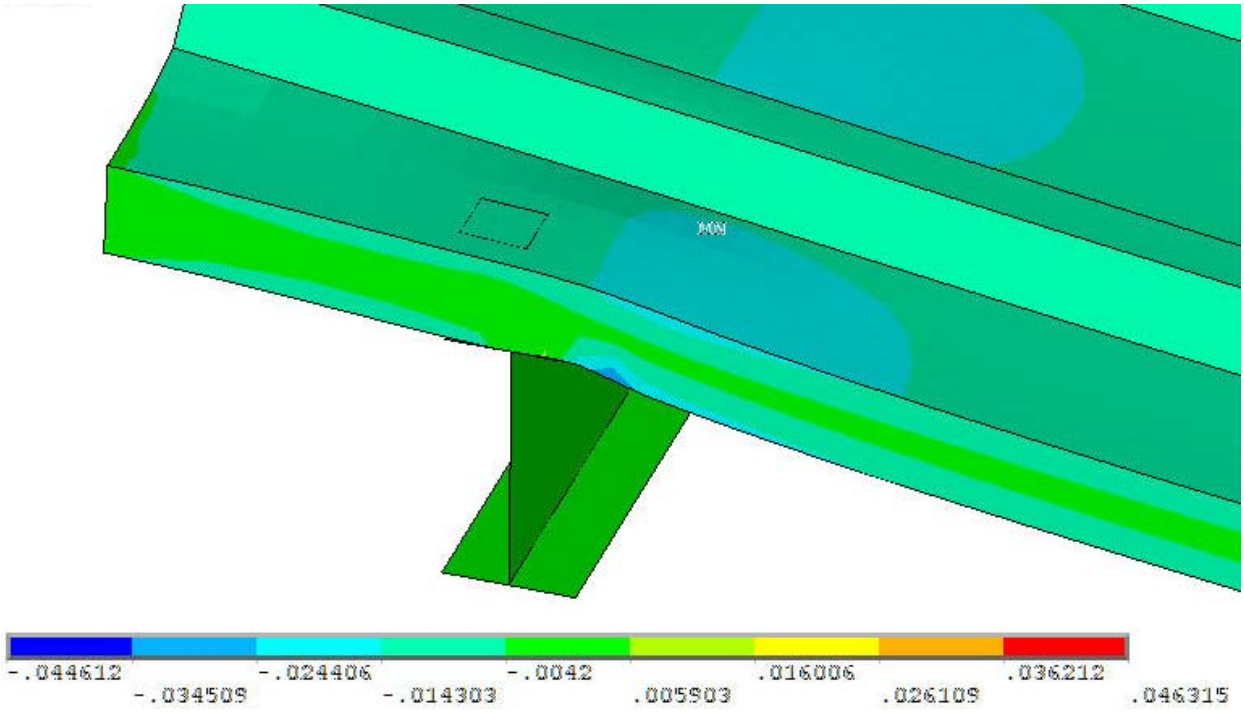

Fig. 11: Deformation at the stage of $c_{\vartheta 1}$

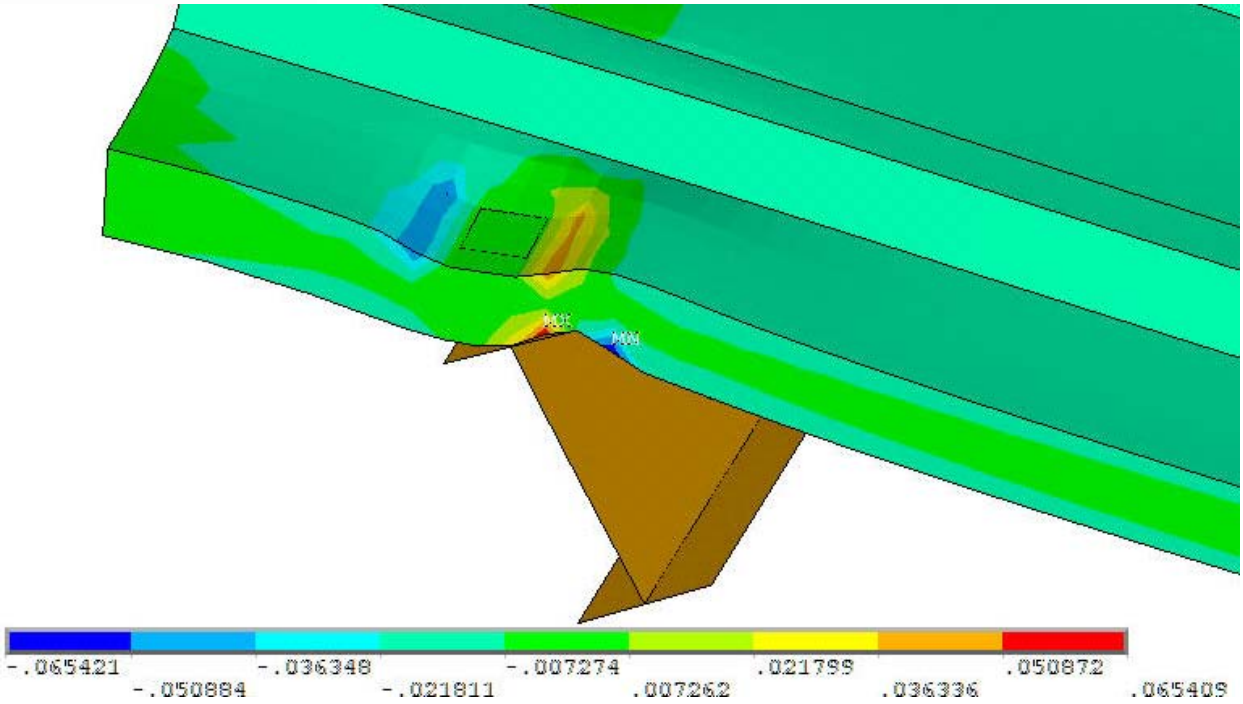

Fig. 12: Deformation at the stage of $c_{\vartheta 2}$

4.3 Stiffness of the core material

To get into-depth knowledge of the influence of the core material on the rotational stiffness finite element calculations were done. These investigations were done for different face geometries and fasteners application: Both wall panels with lightly profiled faces and roof panels with strongly profiled faces were investigated. For roof panels fixing in the upper and lower flange was investigated. All other geometrical and material properties were kept the same. The results are listed in the following tables.

Index i	$E_{C,i}$	$c_{\vartheta 1}$	$c_{\vartheta 2}$
	N/mm²	Nmm/mm	Nmm/mm
1	4	5,9	0,8
2	6	8,2	1,2
3	8	10,5	1,5
4	10	12,5	1,9

Tab. 3: Influence of the stiffness of the core material – wall panels D = 40 mm

Index i	$E_{C,i}$	$c_{\vartheta 1}$	$c_{\vartheta 2}$
	N/mm²	Nmm/mm	Nmm/mm
1	4	9,25	1,1
2	6	13,5	1,6
3	8	17,4	2,0
4	10	21,1	2,5

Tab. 4: Influence of the stiffness of the core material – wall panels D = 120 mm

Index i	$E_{C,i}$	$c_{\vartheta 1}$	$c_{\vartheta 2}$
	N/mm²	Nmm/mm	Nmm/mm
1	4	9,0	0,9
2	6	12,5	1,3
3	8	15,8	1,7
4	10	18,9	2,1

Tab. 5: Influence of the stiffness of the core material – roof panels (fixing in the lower flange)

Index i	$E_{C,i}$	$c_{\vartheta 1}$	$c_{\vartheta 2}$
	N/mm²	Nmm/mm	Nmm/mm
1	4	9,6	2,8
2	6	13,5	3,8
3	8	17,0	4,7
4	10	20,4	5,5

Tab. 6: Influence of the stiffness of the core material – roof panels (fixing in the upper flange)

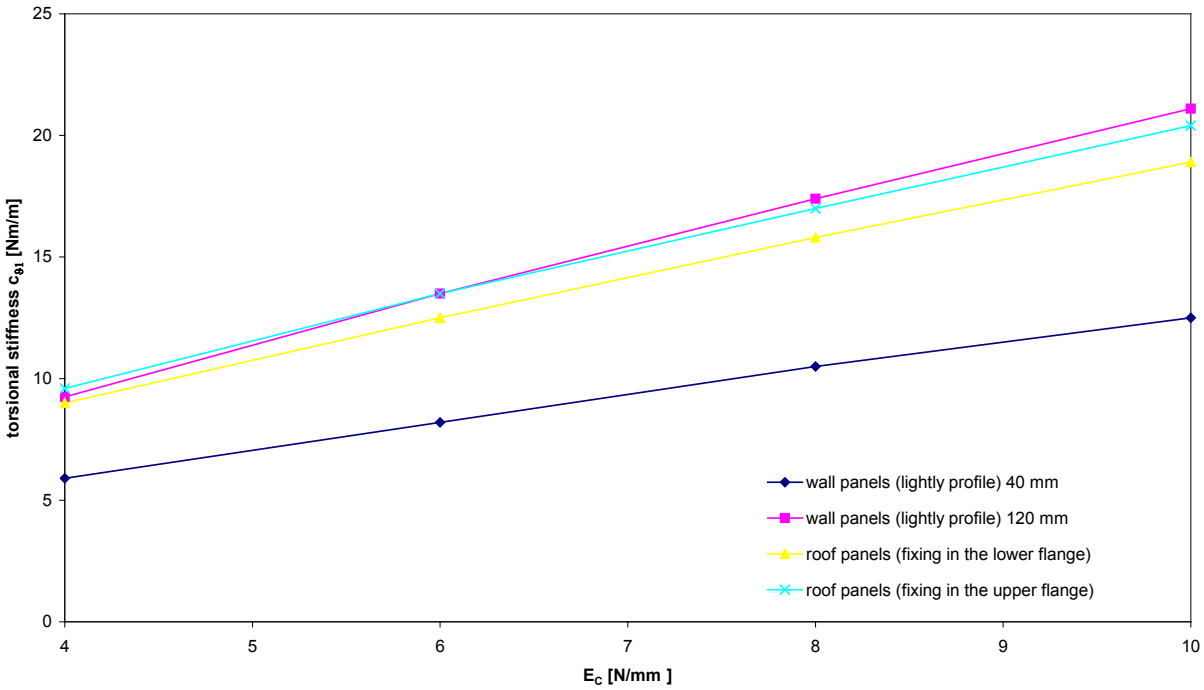

Fig. 13: $c_{\vartheta 1}$ for different elastic modulus of the core

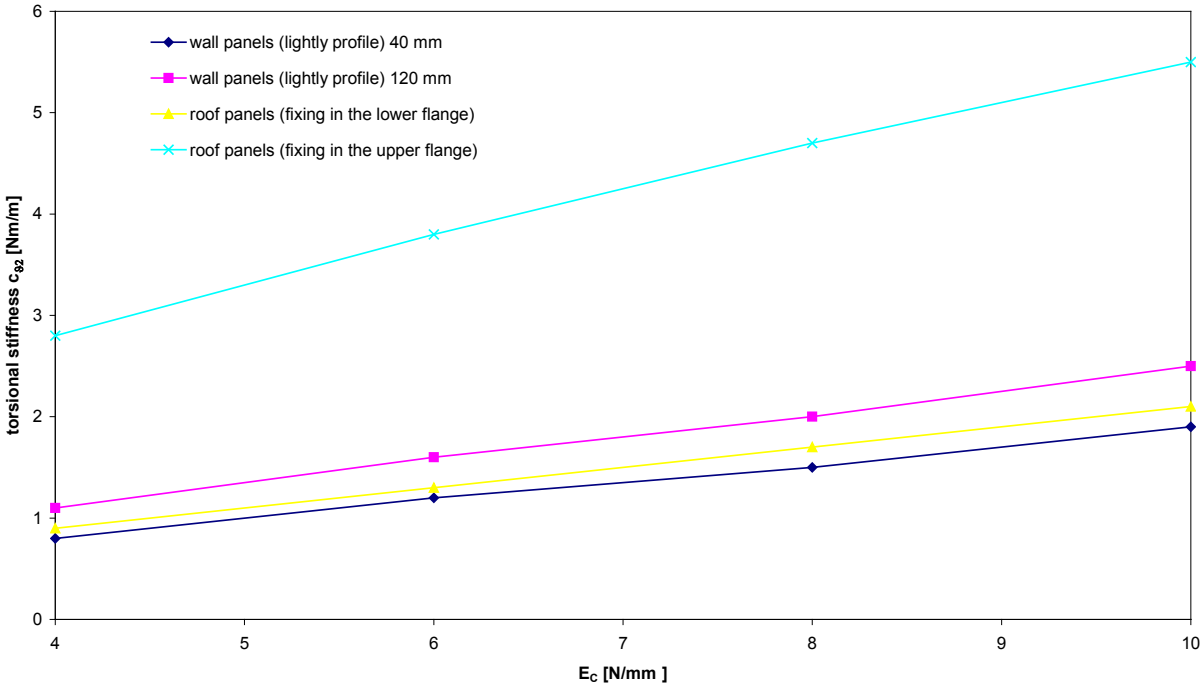

Fig. 14: $c_{\vartheta 2}$ for different elastic modulus of the core

The calculated moment-rotation-curves are shown in the following figures.

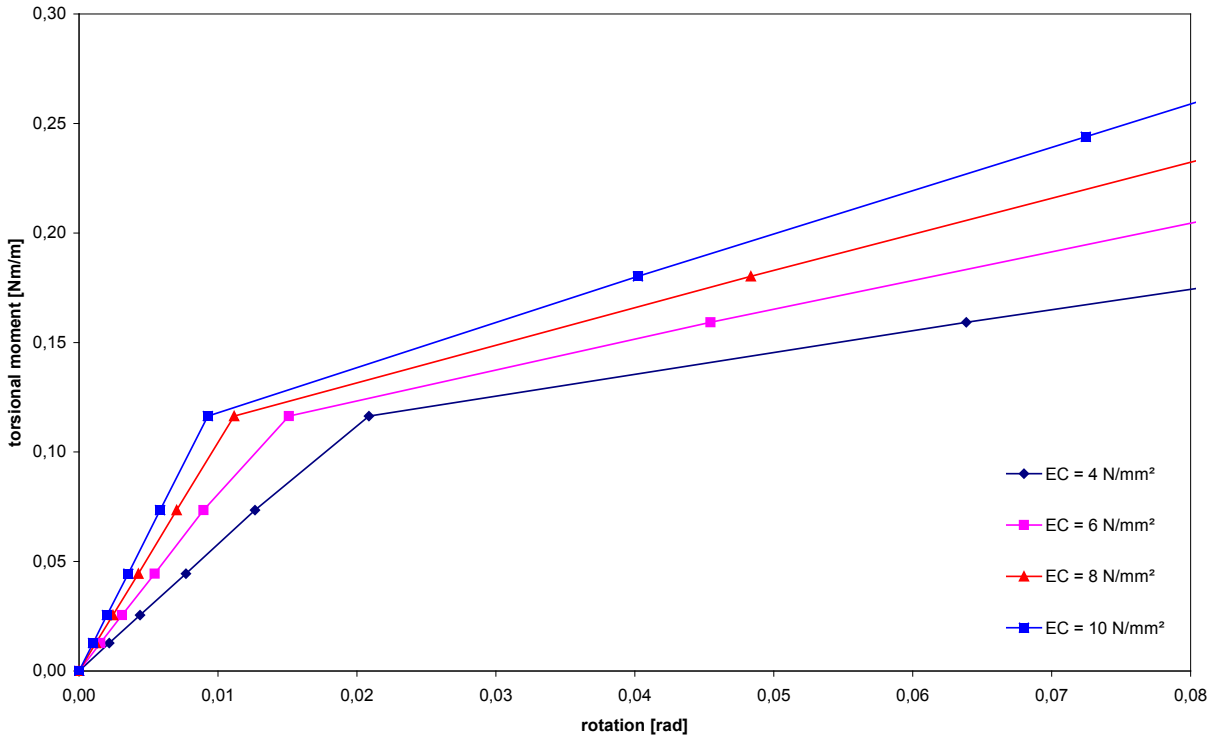

Fig. 15: Moment-rotation-relations for wall panels D = 40 mm

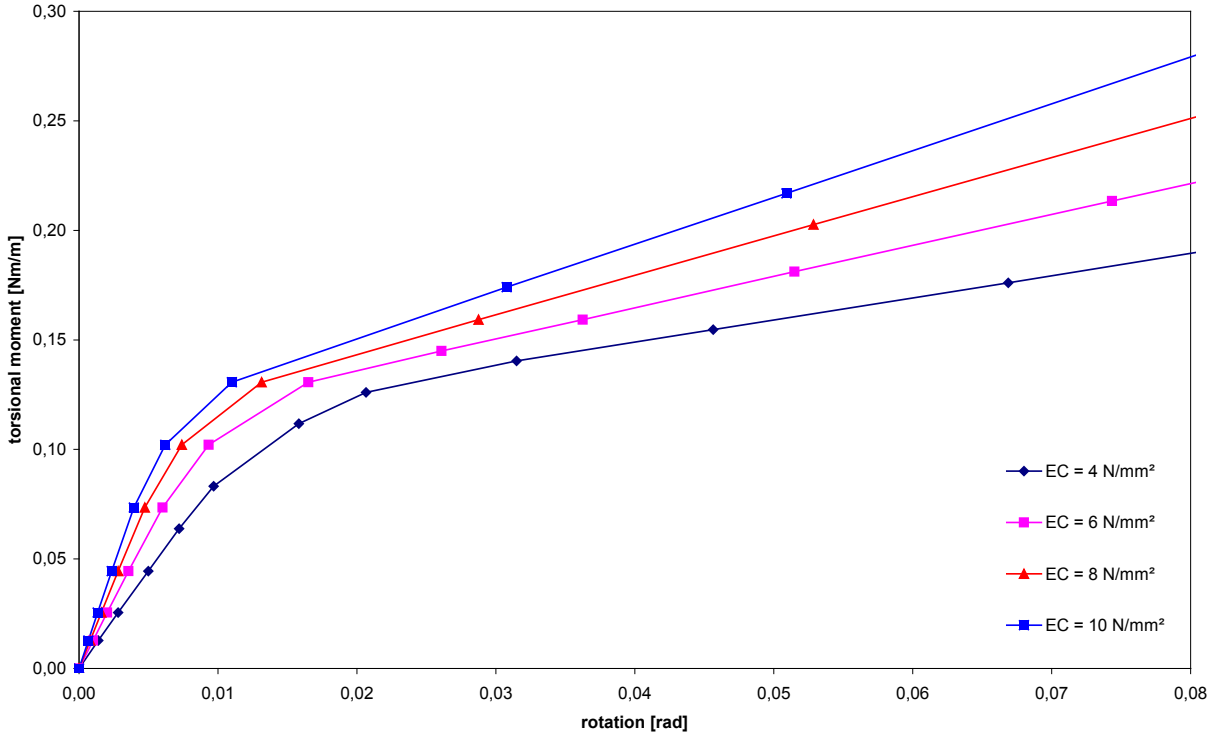

Fig. 16: Moment-rotation-relations for roof panels (fixing in the lower flange)

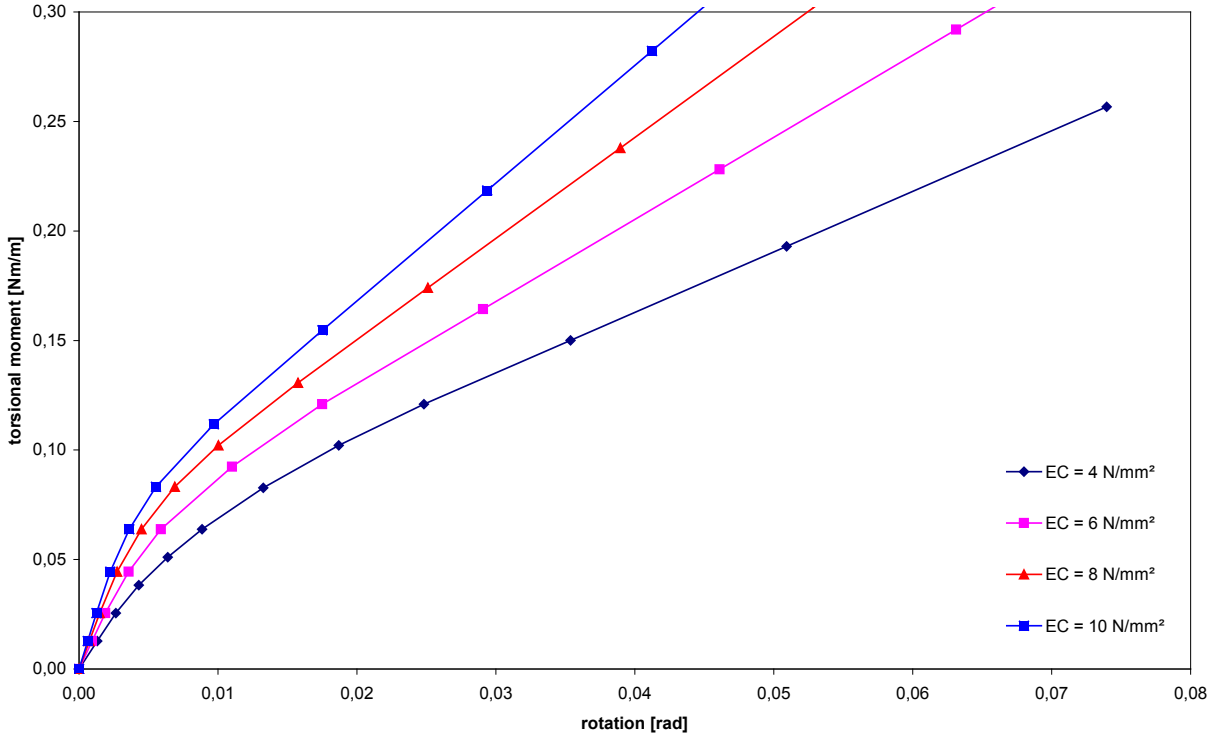

Fig. 17: Moment-rotation-relations for roof panels (fixing in the upper flange)

The increase in torsional stiffness follows the elastic modulus of the core approximately with the power of 0,9. A linear dependency can be assumed. This correlates with the mechanical model presented in chapter 3. Two additional characteristics can be found:

- The change from $c_{\vartheta 1}$ to $c_{\vartheta 2}$ is much sharper for wall panels.
- Fixing in the upper flange increases $c_{\vartheta 2}$ and – to a lower extend - $c_{\vartheta 1}$.

4.4 Stiffness of the face material

Sandwich panels are also produced with faces made of aluminium or GFRP instead of steel. Therefore finite element calculations were done to study the influence of the lower elastic modulus on stiffness. Two parametric studies were done: The first one being a more general comparison with fictitious materials for the inner face (and steel for the outer face), the second one with material laws for GFRP and Aluminium, also including two different material models for aluminium.

Fig. 18 and Tab. 7 show the increase of $c_{\vartheta 1}$ with increasing elastic modulus E_{F2} of the inner face. There is a significant increase for small values of E_{F2}, but for medium to higher values there is no significant increase in the value $c_{\vartheta 1}$.

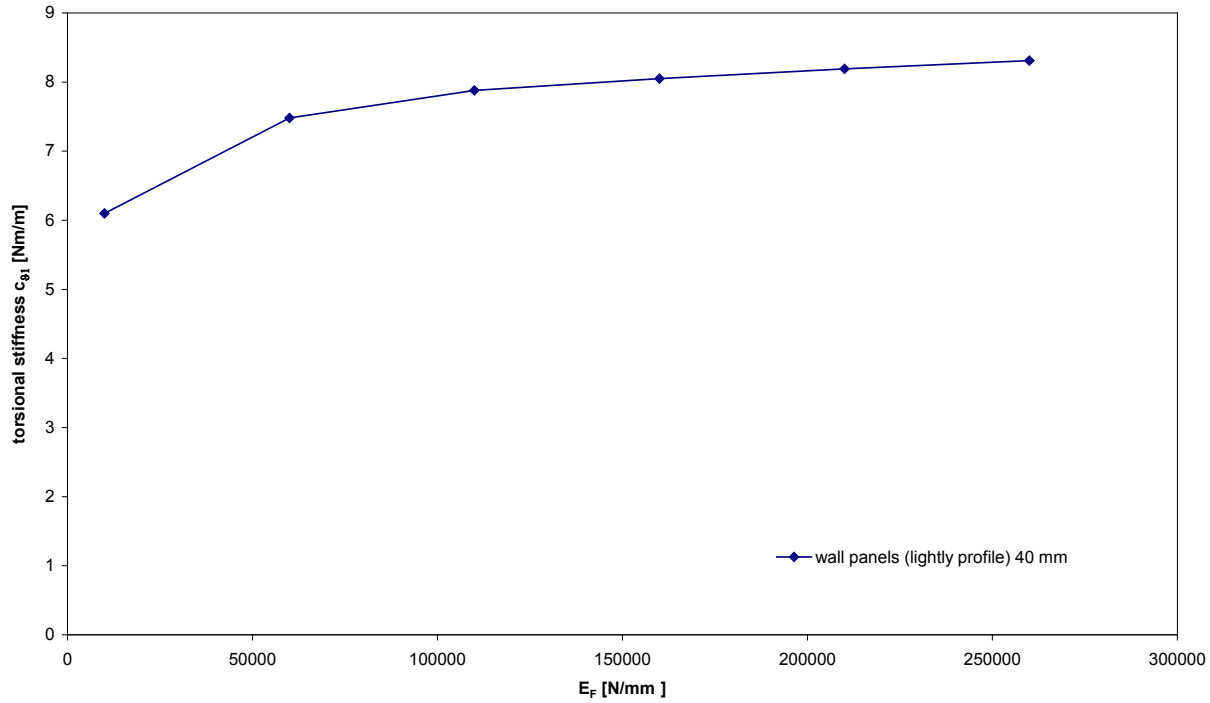

Fig. 18: Increase of $c_{\vartheta 1}$ with width E_F

Index i	E_F	$c_{\vartheta 1}$
	N/mm²	Nmm/mm
1	10000	6,1
2	60000	7,5
3	110000	7,8
4	160000	8,1
5	210000	8,2
6	260000	8,3

Tab. 7: Effect of elastic modulus of the faces

The calculations done in the second study are listed in Tab. 8.

Index i	Face material	E_F	Material law	$f_{y1/2}$	$t_{1/2}$
		N/mm²		N/mm²	mm
1	steel	210000	Linear elastic/ideal plastic	320	0,7
2	steel	210000	Linear elastic/ideal plastic	190	0,7
3	aluminium	70000	Linear elastic/ideal plastic	190	0,7
4	aluminium	70000	Linear elastic/hardening	190	0,7
5	GFRP	7000	Linear elastic	190	0,7
6	GFRP	7000	Linear elastic	80	0,7

Tab. 8: Calculations to determine the influence of the stiffness of the face material

To allow better comparison, a constant thickness of 0,7 mm was used. The calculated moment-rotation-curves are shown in Fig. 19.

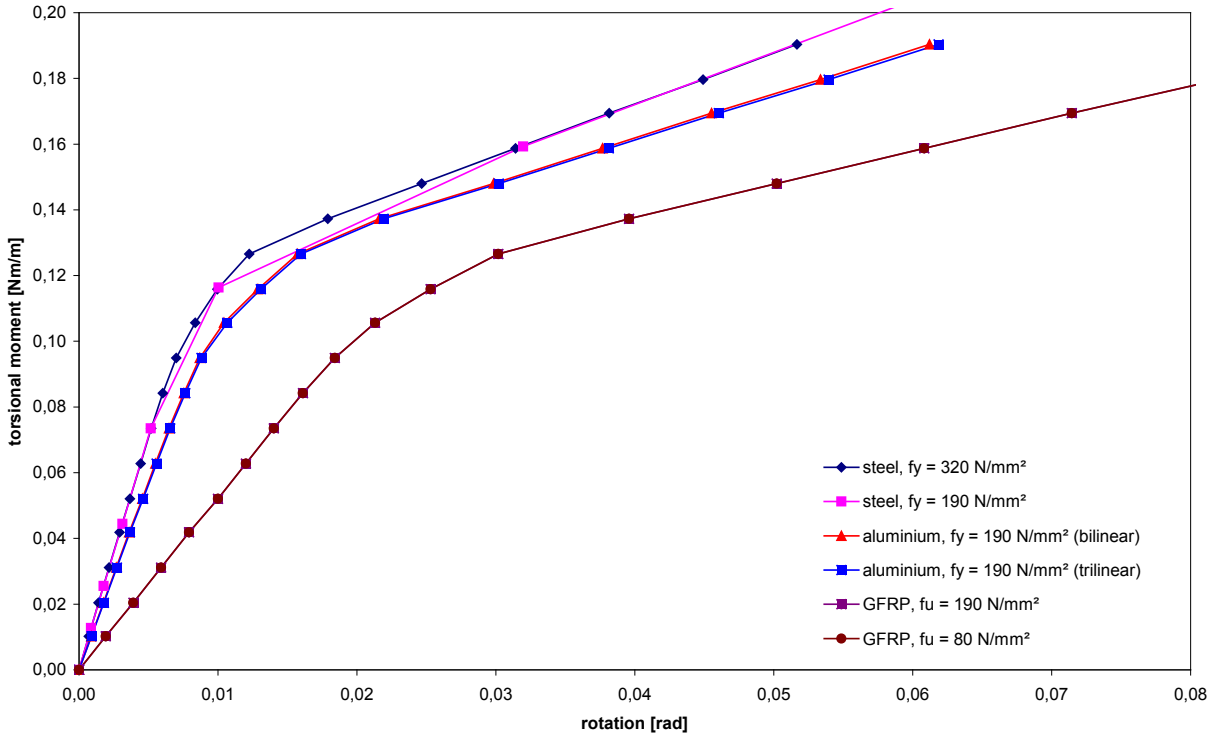

Fig. 19: Moment-rotation curves for faces with different elastic modulus

The following table lists the results for the different calculations. The rations of the elastic modulus (both linear and of the form of the forth root) are listed for comparison.

Index i	$E_{F1/2}$	$c_{\vartheta 1}$	$c_{\vartheta 2}$
	N/mm²	Nmm/mm	Nmm/mm
1	210000	14,7	1,6
2	210000	14,6	1,6
3	70000	11,6	1,3
4	70000	11,4	1,3
5	7000	5,3	1,0
6	7000	5,3	1,0

Tab. 9: Effect of elastic modulus of the faces

It can be seen that there is an approximate decrease of the values $c_{\vartheta 1}$ and $c_{\vartheta 2}$ stiffness with the power 0,25. This is coming from the model of the beam on an elastic foundation. Despite the theoretical model does not include the stiffness of the faces, there is an influence. In fact, there is no influence of the strength. Obviously for metallic materials such as steel and alumin-

ium the influence of $E_{F1/2}$ can be neglected because the differences lay within the scatter of $c_{\vartheta 1}$ obtained with tests. For GFRP an appropriate reduction factor is necessary.

4.5 Width b of the flange of the beam

Numerical investigations were done to check the different powers for the calculation of the influence of the width b when calculating the torsional stiffness. These investigations were done for different face geometries and fasteners application: Both wall panels with lightly profiled faces and roof panels with strongly profiled faces were investigated. For roof panels fixing in the upper and lower flange was investigated. All other geometrical and material properties were kept the same. The results are listed in the following tables.

Index i	b_i	$c_{\vartheta 1}$			$c_{\vartheta 2}$		
	mm	Nmm/mm			Nmm/mm		
Panel thickness		40	120	240	40	120	240
1	82	5,8	9,1	10,0	0,8	1,1	1,1
2	160	11,2	23,9	29,0	2,4	4,0	4,2
3	240	-	42,3	59,4	-	8,6	10,4

Tab. 10: Influence of the width b – wall panels with different thickness

Index i	b_i	$c_{\vartheta 1}$		$c_{\vartheta 2}$	
	mm	Nmm/mm		Nmm/mm	
Panel thickness		40	120	40	120
1	82	9,1	10	0,9	1,1
2	160	24,3	28,5	2,9	4,1
3	240	45,6	56,8	-	9,6

Tab. 11: Influence of the width b – roof panels (fixing in the lower flange) with different thickness

Index i	b_i	$c_{\vartheta 1}$	$c_{\vartheta 2}$
	mm	Nmm/mm	Nmm/mm
Panel thickness		40	40
1	82	9,6	2,8
2	160	27,1	9,7
3	240	50,4	-

Tab. 12: Influence of the width b – roof panels (fixing in the upper flange)

Both mechanical models assume an increase of the values $c_{\vartheta 1}$ and $c_{\vartheta 2}$ with the square of b. For thin wall panels, $c_{\vartheta 1}$ increases only linear with b. With an increasing depth of profiling, the value of the power increases to 1,5 to 1,7. The actual lever arm is smaller than b because of the indentation. Effects of bending stiffness of the panel seem to interact with the effects of

the width of the beam. With the exception of very thin wall and roof panels, $c_{\vartheta 2}$ increases with the square of b. For better comparison, the values $c_{\vartheta 1}$ and $c_{\vartheta 2}$ are plotted above the width b.

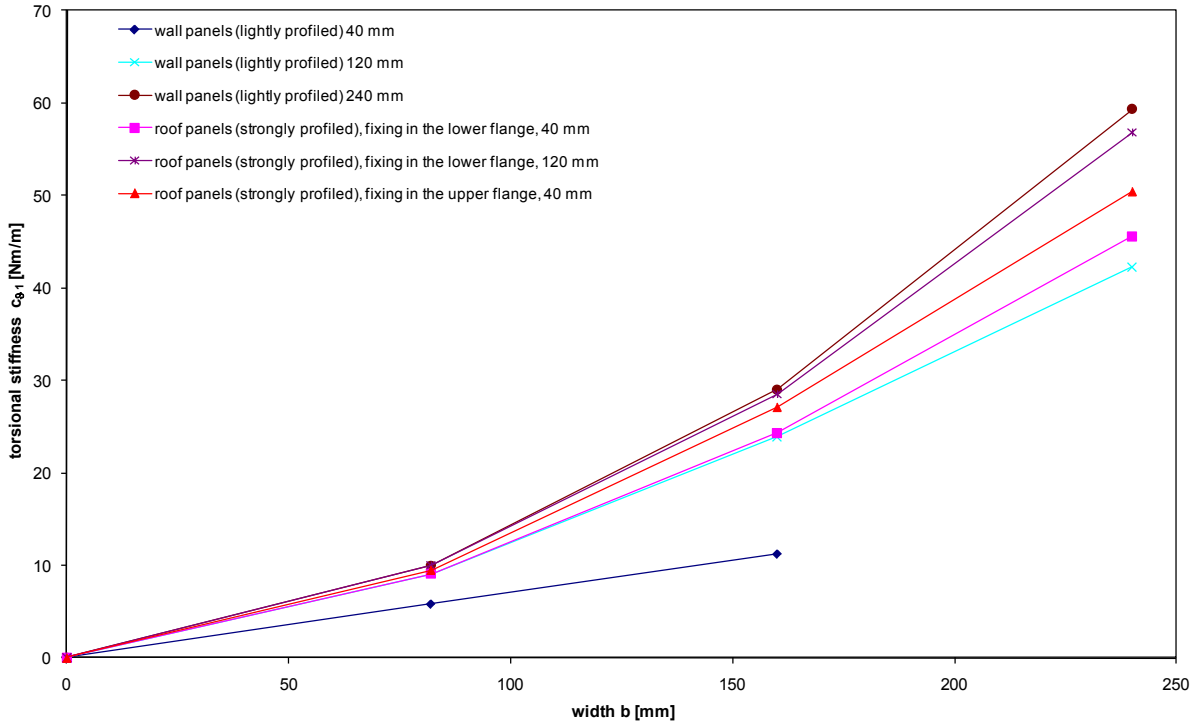

Fig. 20: Increase of $c_{\vartheta 1}$ with width b

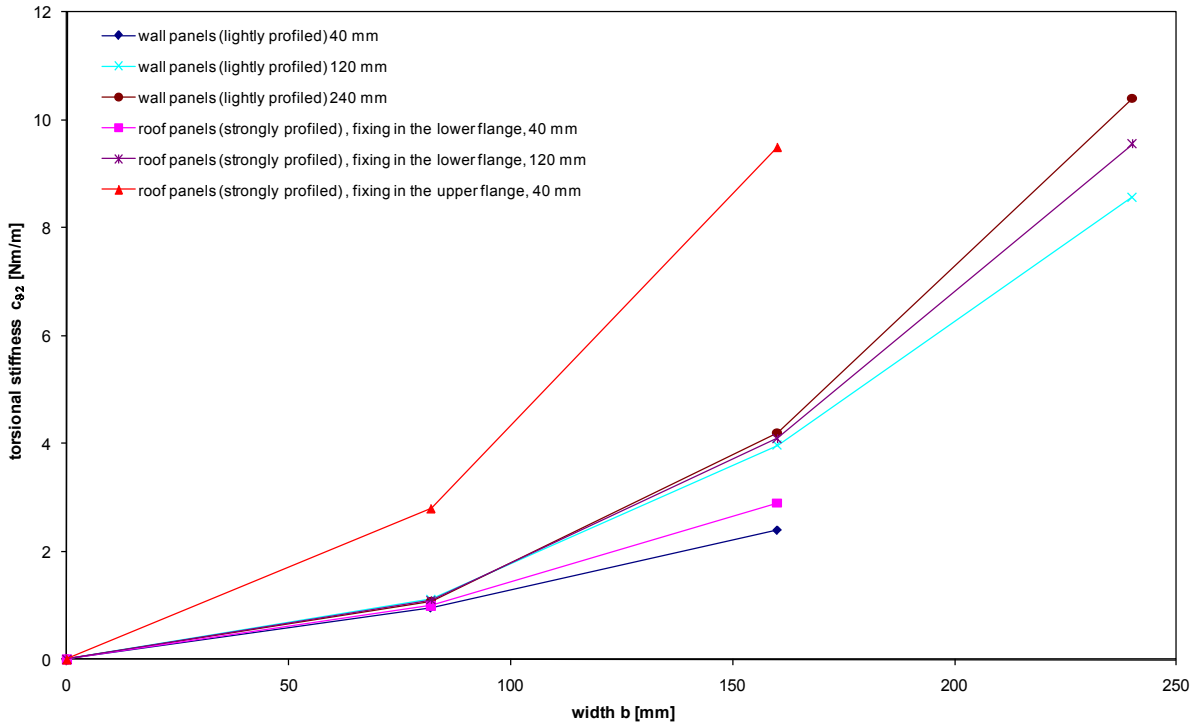

Fig. 21: Increase of $c_{\vartheta 2}$ with width b

4.6 Thickness of the panels

The thickness of the panel influences the rotational stiffness. As seen in the chapter before, the dependence of the rotational stiffness from the width b varies with thickness D. This is due to effects of bending stiffness overlying with the effects of indentation. Therefore some numerical calculations were done to estimate this effect. The following figures show the increase of rotational stiffness of the connection of wall panels with thickness D. For thick panels, the value tends to an end value for $c_{\vartheta 1}$ and $c_{\vartheta 2}$. For this final value, the nearly quadratic dependency of $c_{\vartheta 1}$ from b applies. It can also be seen, that this effect can be neglected for roof panels.

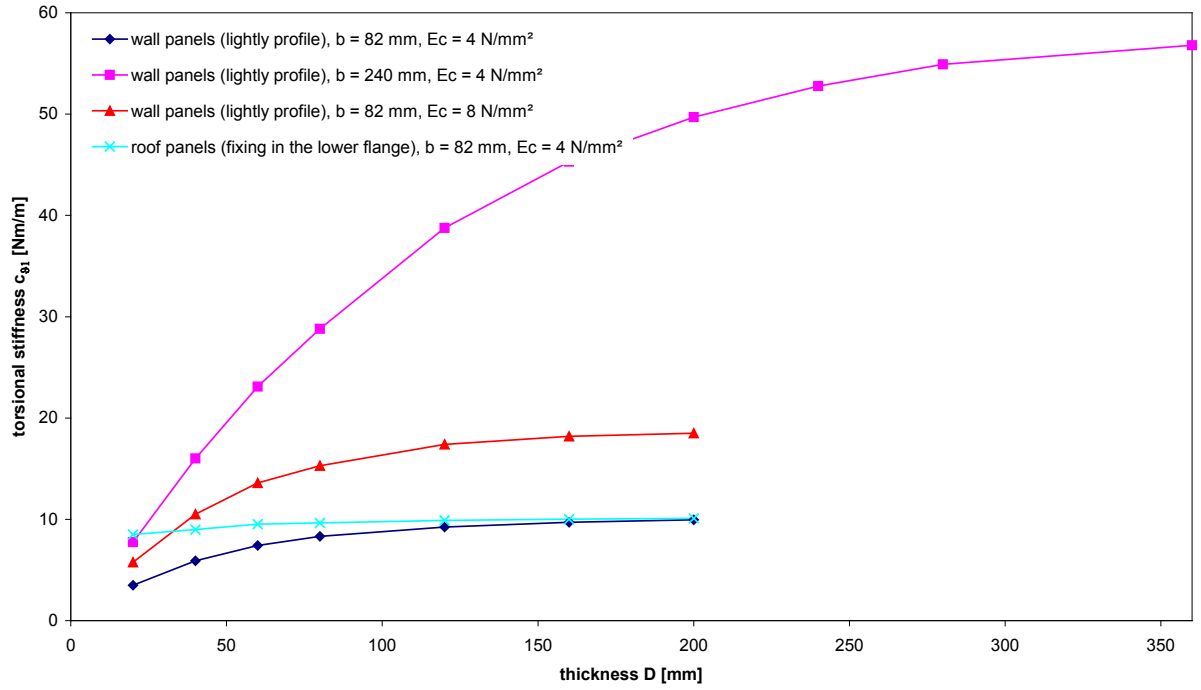

Fig. 22: Increase of $c_{\vartheta 2}$ with thickness D

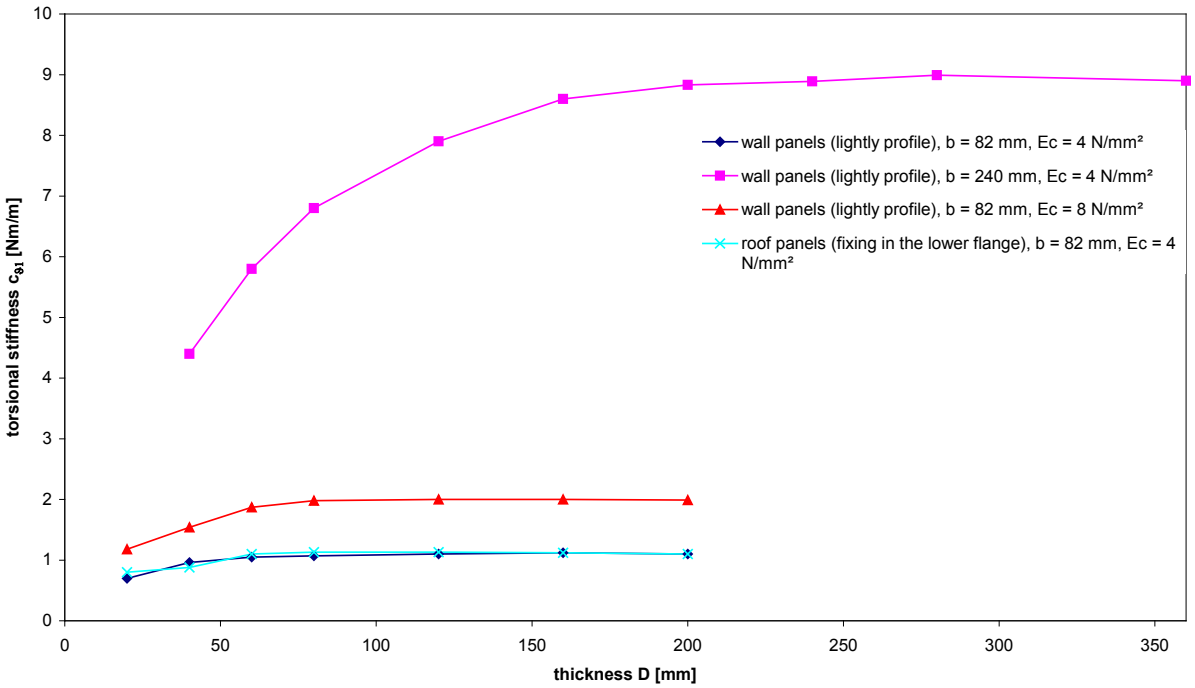

Fig. 23: Increase of $c_{\vartheta 2}$ with thickness D

4.7 Fixing in the upper or lower flange of roof panels

When comparing Fig. 16 and Fig. 17 it can be see that a fixing in the upper flange increases $c_{\vartheta 2}$ and – to a lower extend – also $c_{\vartheta 1}$.

Index i	$E_{C,i}$	$c_{\vartheta 1}$	
		fixing in the lower flange	fixing in the upper flange
	N/mm²	Nmm/mm	
1	4	9,0	9,6
2	6	12,5	13,5
3	8	15,8	17,0
4	10	18,9	20,4

Tab. 13: Influence of the fixing of roof panels on $c_{\vartheta 1}$

Index i	E_C	$c_{\vartheta 2}$	
		fixing in the lower flange	fixing in the upper flange
	N/mm²	Nmm/mm	
1	4	0,9	2,8
2	6	1,3	3,8
3	8	1,7	4,7
4	10	2,1	5,5

Tab. 14: Influence of the fixing of roof panels on $c_{\vartheta 2}$

4.8 Depth of profiling of the outer face

With increasing depth of profiling, the stiffness of the outer face and of the panel increases. There is also an effect on the indentation stiffness for the washer. The following tables list the results of the calculations.

Index i		$c_{\vartheta 1}$	$c_{\vartheta 2}$
	mm	Nmm/mm	Nmm/mm
1	2	5,9	0,8
2	5	6,5	0,9
3	10	7,3	0,9
4	20	8,0	1,0
5	30	8,4	1,0
6	45	9,1	1,0
7	50	9,2	1,0

Tab. 15: Influence of the width b – roof panels (fixing in the lower flange)

Index i	h	$c_{\vartheta 1}$	$c_{\vartheta 2}$
	mm	Nmm/mm	Nmm/mm
1	2	5,9	1,5
2	5	6,7	2,0
3	10	7,7	2,5
4	20	8,7	2,6
5	30	9,1	2,7
6	45	9,6	2,8
7	50	9,7	2,8

Tab. 16: Influence of the width b – roof panels (fixing in the upper flange)

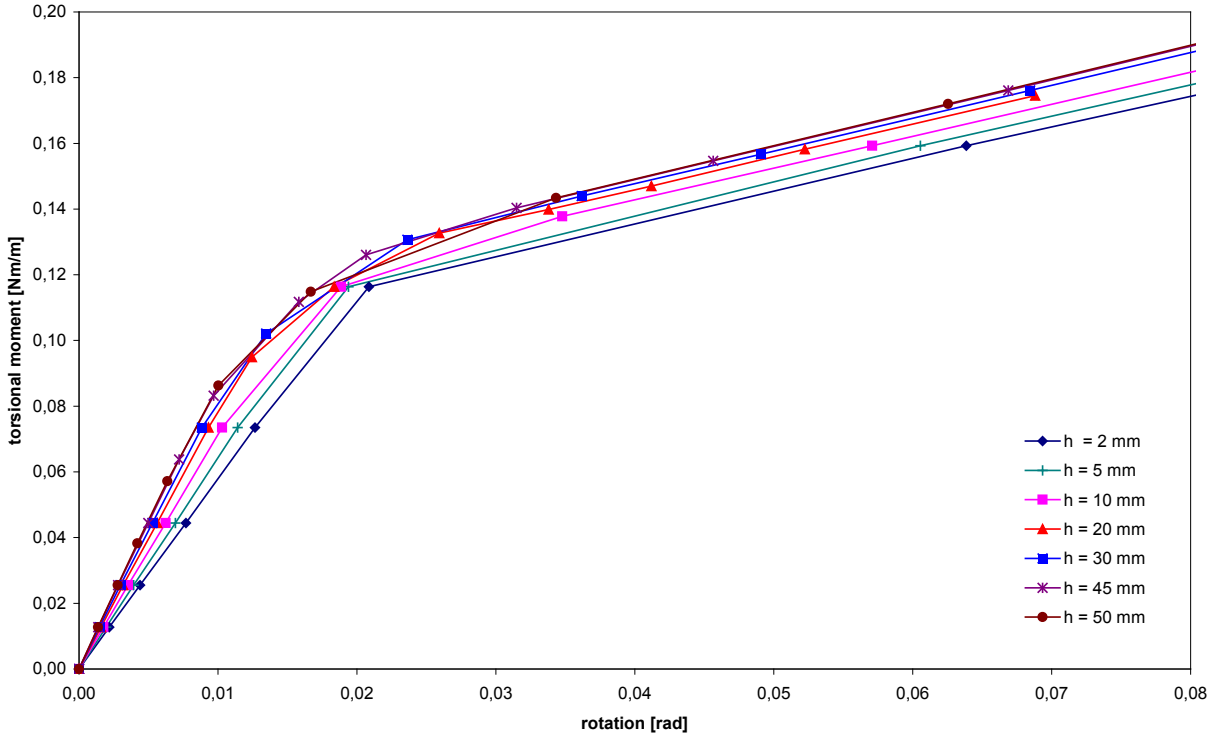

Fig. 24: Moment-rotation-relation for different depths h (fixing in the lower flange)

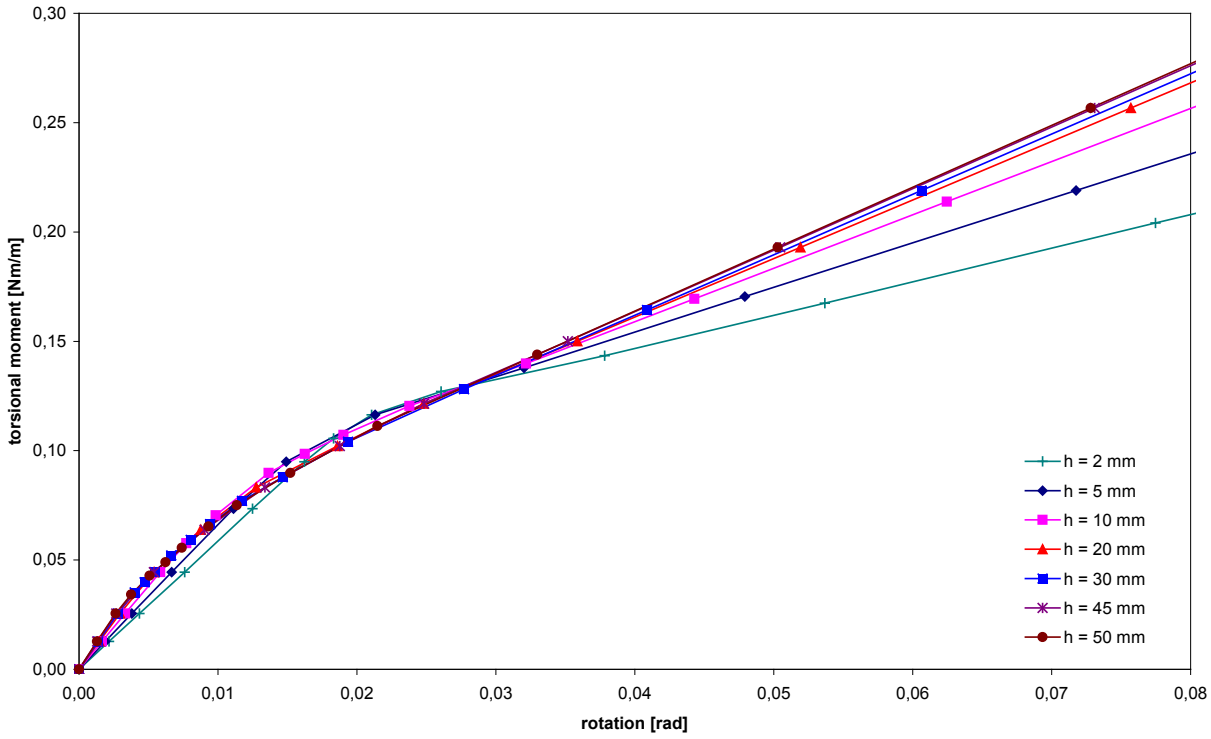

Fig. 25: Moment-rotation-relation for different depths h (fixing in the upper flange)

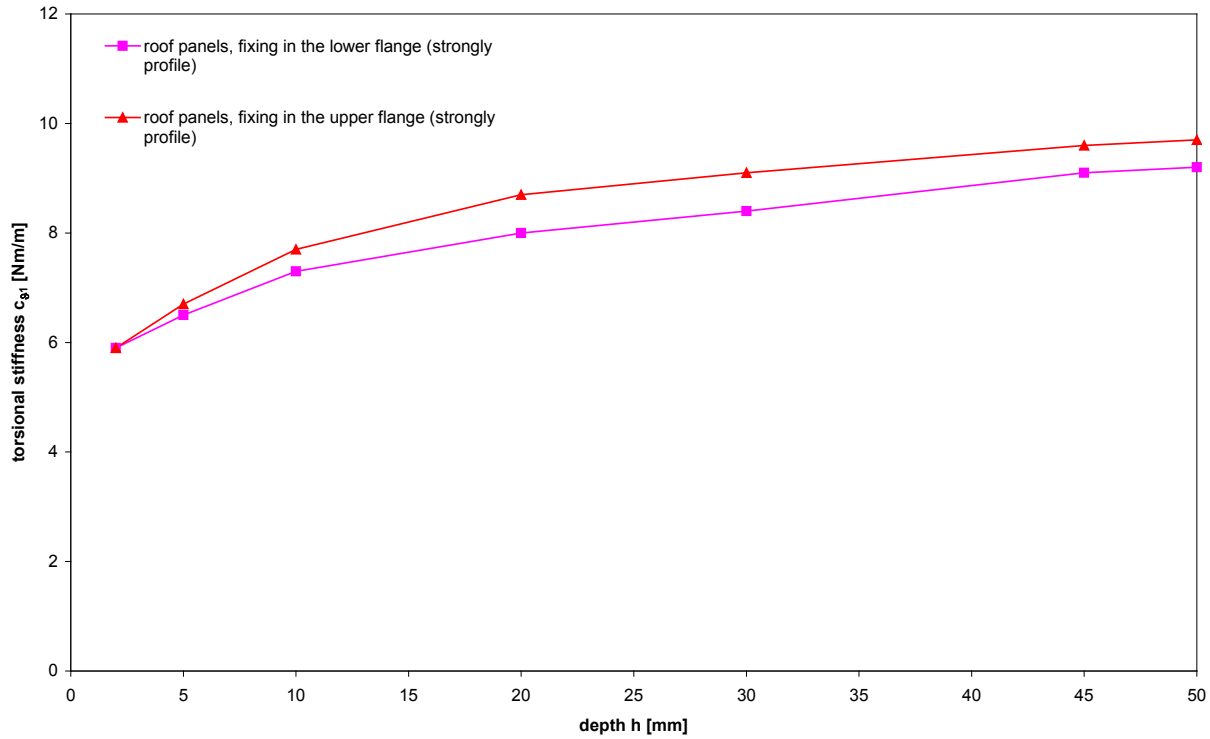

Fig. 26: Increase of $c_{\vartheta 1}$ with depth h

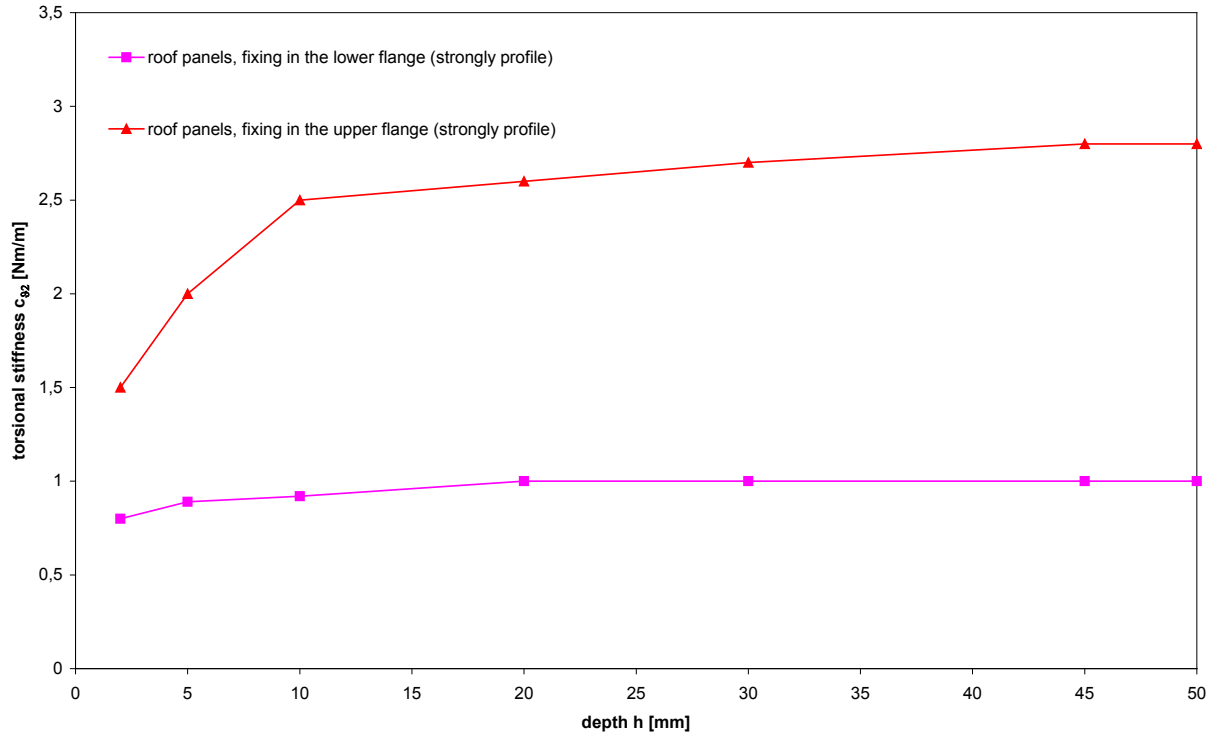

Fig. 27: Increase of $c_{\vartheta 2}$ with depth h

An increase in depth leads to small increase in $c_{\vartheta 1}$ because the panel stiffness increases: The web of the outer face can transfer shear forces. A much large increase can be found for $c_{\vartheta 2}$ when the fasteners are mounted in the upper flange: For fixing in the upper flange, the in-

creasing depth reduces the penetration of the fastener, leading also to an increase in rotational stiffness.

In fact, the increase of $c_{\vartheta 1}$ and $c_{\vartheta 2}$ is large for small values of the depth h, but for higher values there is nearly no influence. This allows to sum up all test results in the two groups “wall application” (depth $h \leq 10$ mm) and “roof application” (depth $h > 10$ mm).

4.9 Type of loading

The results listed in Tab. 12 allow for a comparison between the results obtained for downward and uplift loading. It has to be pointed out that these values were obtained for rather low values of loading where the gap between the inner face occurring under uplift loading was rather small and could be closed after some rotation.

application		$c_{\vartheta 1}$	$c_{\vartheta 2}$
	mm	Nmm/mm	Nmm/mm
Wall	Downward	5,5	0,8
	uplift	0,2	0,5
Roof, fixing in the lower flange	Downward	9,2	2,1
	uplift	0,2	0,7
Roof, fixing in the upper flange	Downward	9,7	3,3
	uplift	1,6	2,4

Tab. 17: Influence of the type of loading

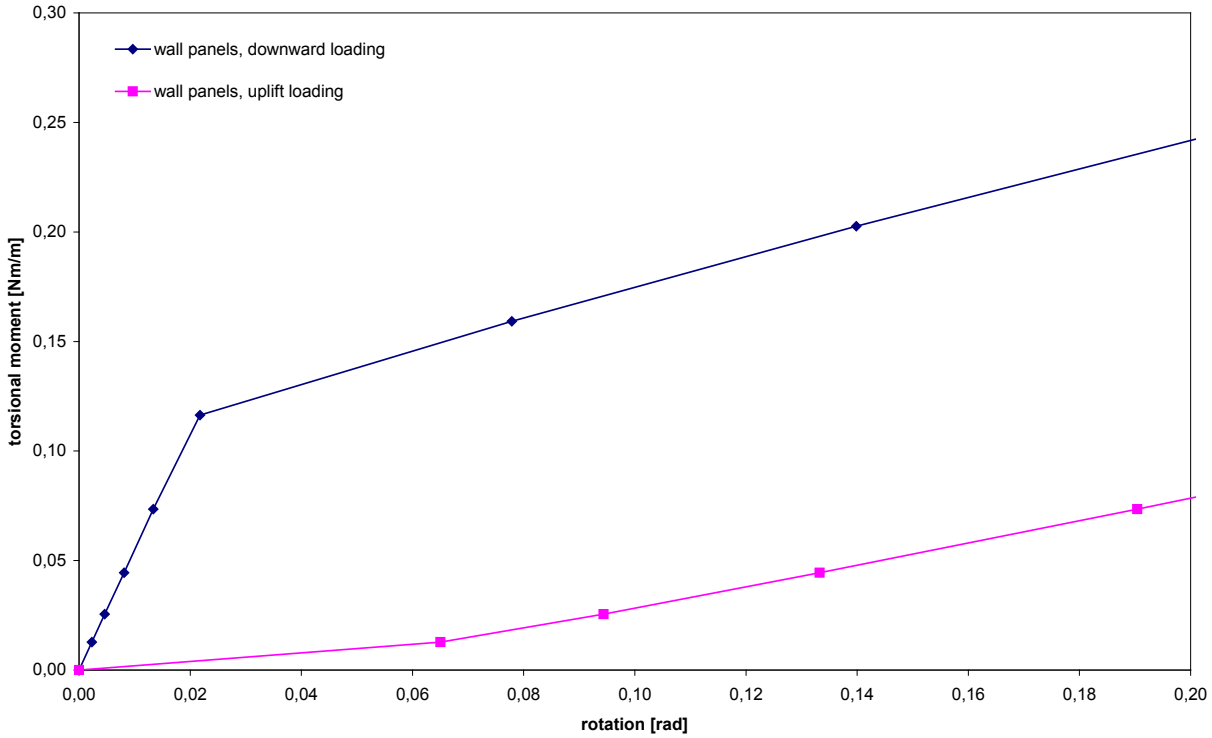

Fig. 28: Influence of the type of loading – wall panels

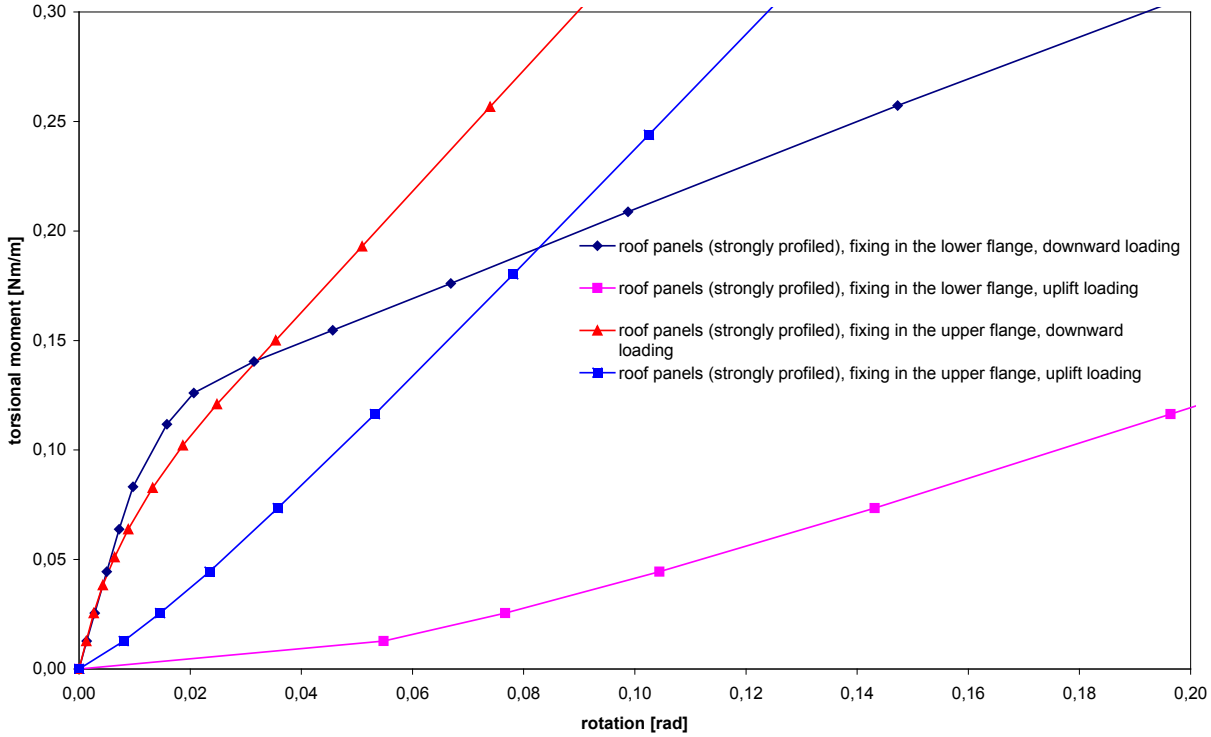

Fig. 29: Influence of the type of loading – roof panels

Uplift load causes an indentation of the fastener and a gap between the upper flange and the inner face of the beam. Therefore for uplift load, no rotational restraint can be assured. If indentation is reduced (for example, for fixing in the upper flange, where the webs of the outer face give additional stiffness), a torsional restraint exist, but is hard to quantify because of the influence of the additional parameters.

4.10 Summary

The results of the numerical investigations can be summarized:

- Both $c_{\vartheta 1}$ and $c_{\vartheta 2}$ increase with Young's modulus E_C of the core material with the power of 0.9. The approximation by a linear function is justified.
- For panels with two flat or lightly profiled faces (wall panels) both $c_{\vartheta 1}$ and $c_{\vartheta 2}$ depend on the thickness D of the panels. $c_{\vartheta 1}$ and $c_{\vartheta 2}$ increase with the thickness D. They converge to the value of the panel with a strongly profiled outer face (usually roof panels) with similar arrangement of the fasteners.
- $c_{\vartheta 1}$ increases with the bending stiffness $(EI)_{F2}$ of the inner face with the power of 0,1. The influence of this stiffness can therefore be neglected for the common parameter range (faces made of steel with thickness 0,38 mm $\leq t_K \leq$ 0,71 mm, faces made of aluminium with 0,50 mm $\leq t \leq$ 0,65 mm). For faces made of GFRP a reduction factor c_F is required. As expected there is no influence of $(EI)_{F1}$ of the outer face on $c_{\vartheta 1}$ such that $(EI)_{F1}$ can also be disregarded.

$c_{\vartheta 2}$ increases with the bending stiffness $(EI)_{F1}$ of the outer face with the power less than 0,1 so the same applies as for $c_{\vartheta 1}$. There is no significant increase of $c_{\vartheta 2}$ with increasing bending stiffness $(EI)_{F2}$ of the inner face. This justifies the mechanical model introduced above that $c_{\vartheta 2}$ only depends on the core material and the type of profiling of the outer face.

- $c_{\vartheta 1}$ does not increase with the square of b but with the power of 1,3 (thin wall panels) to 1,7 (thick wall panels): The actual lever arm is smaller than b because of the indentation and because of bending of the panel itself, leading to an effect of thickness D on $c_{\vartheta 1}$. $c_{\vartheta 2}$ increases with the square of b.
- Torsional restraint is much smaller with uplift loading than with downward loading and can only be applied for small uplift loads. For higher loads, the gap between the flange of the beam and the inner face is increasing too much cannot be closed by a rotation of the beam.

5 Experimental investigations

5.1 Preliminary remarks

The experimental tests are described in report D3.2 – part 1. Tab. 18 depicts a compilation of all tests performed. At this, the application, loading and materials are listed.

No.	Application	Loading	Core material	Face material
01	wall	downward	EPS	steel
02	wall		EPS	GFRP
03	wall		PUR	aluminium
04a	roof		PUR	aluminium
04b	roof		PUR	aluminium
05	roof		MW	steel
06	wall		PUR	steel
07	wall	uplift	PUR	steel
08	wall		PUR	steel
09	wall		MW	steel
10	wall		MW	Steel
11	wall		EPS	Steel
12	roof		PUR	steel
13	roof		PUR	steel
14	roof		MW	steel
16	roof	downward	PUR	steel
16k	roof		PUR	steel
17	roof		MW	steel
18k	roof	uplift	PUR	steel
18ok	roof		PUR	steel
19	roof		PUR	steel

Tab. 18: Compilation of performed tests on torsional restraint

5.2 Sandwich panels

Investigations on roof and wall panels of different producers were performed. In addition to sandwich panels with polyurethane foam core, panels with a core made of mineral wool or EPS were investigated as well. The thicknesses of the core layers varied between 40 mm and 80 mm. The face layers of the panels were made of steel, aluminium or glass-fibre reinforced plastics (GFRP). The thickness varied between 0.40 mm and 0.50 mm for steel faces, and between 0.50 mm and 0.70 mm for the aluminium faces. The thickness of the GFRP-faces was 1,8 mm. Tab. 19 gives a compilation of parameter combinations for the tested sandwich panels.

No.	Core material	Core thickness	Face material	Face thickness
01	EPS	60	steel	0,60 / 0,60
02	EPS	60	GFRP	1,80 / 1,80
03	PUR	60	aluminium	0,65 / 0,65
04a	PUR	58	aluminium	0,70 / 0,50
04b	PUR	58	aluminium	0,70 / 0,50
05	MW	80	steel	0,60 / 0,60
06	PUR	80	steel	0,50 / 0,50
07	PUR	80	steel	0,50 / 0,50
08	PUR	80	steel	0,50 / 0,50
09	MW	80	steel	0,50 / 0,50
10	MW	80	Steel	0,50 / 0,50
11	EPS	60	Steel	0,60 / 0,60
12	PUR	40	steel	0,50 / 0,40
13	PUR	40	steel	0,50 / 0,40
14	MW	80	steel	0,60 / 0,60
16	PUR	40	steel	0,50 / 0,40
16k	PUR	80	steel	0,50 / 0,40
17	MW	40	steel	0,50 / 0,40
18k	PUR	40	steel	0,50 / 0,40
18ok	PUR	40	steel	0,50 / 0,40
19	PUR	40	steel	0,50 / 0,40

Tab. 19: materials and nominal dimensions of the sandwich panels tested

5.3 Beam sections and fasteners

Investigations were performed with hot-rolled medium flange I-beams of type IPE 160 according to DIN 1025-5 and with hot-rolled wide flange I-beams HE 160 B according to DIN 1025-2.

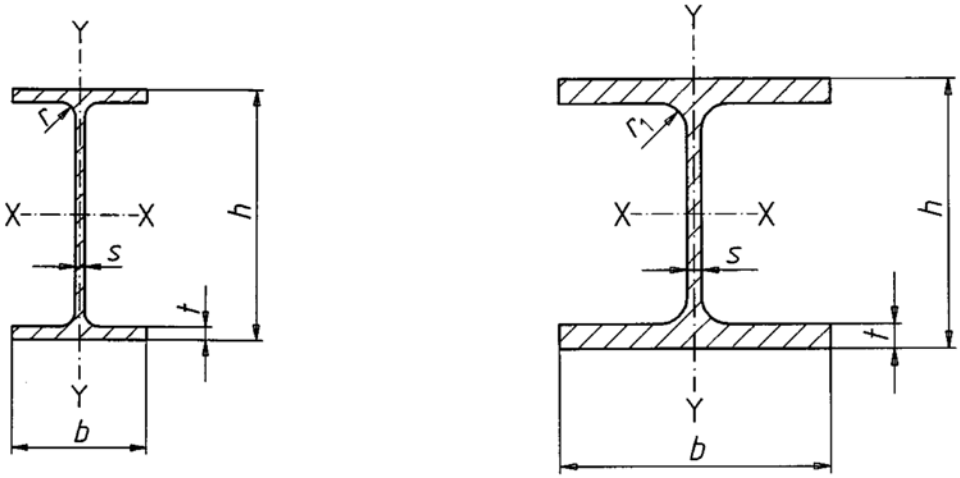

b = 160 mm
h = 82 mm
s = 5 mm
t = 7,4 mm
r = 9 mm

h = 160 mm
b = 160 mm
s = 8 mm
t = 13 mm
r_1 =15 mm

Fig. 30: Beam sections investigated

For fastening the sandwich panels with the beam sections, self-tapping screws made of stainless steel of type Würth FABA Typ BZ 6.3xL were used with seal washers 16 mm. Mutual fastening of the sandwich panels for roof application in the longitudinal joint was done with self-drilling screws of type Würth Zebra Piasta 4,8x22 with undercut and with seal washers 14 mm. The fasteners applied are presented in Fig. 31.

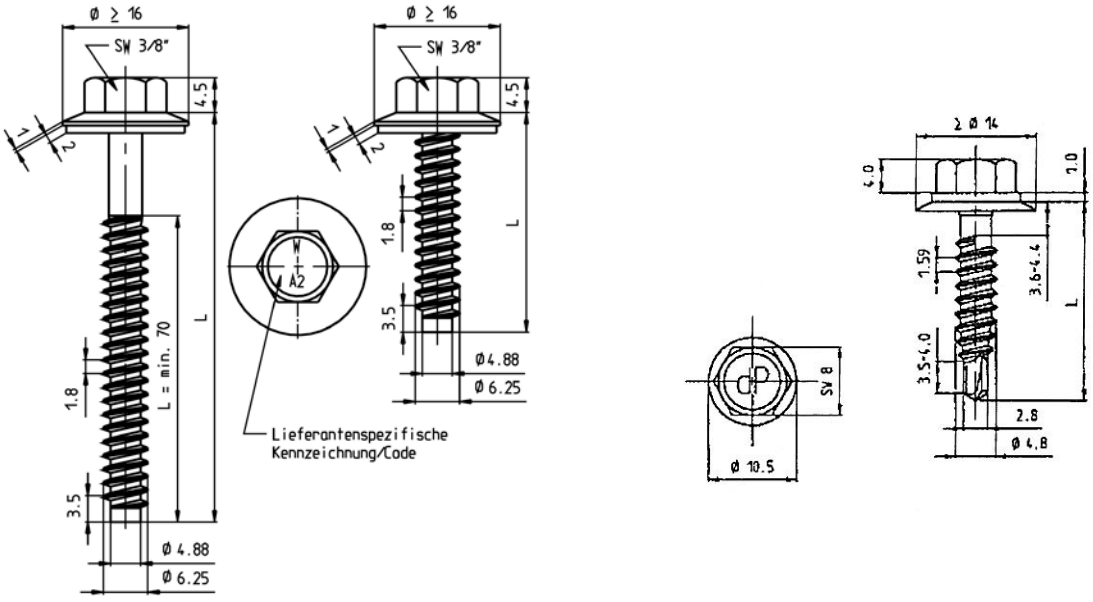

Fig. 31: Fasteners

Several tests were performed with sandwich panels for roof application with fixing in the upper flange by using saddle washers, Fig. 32.

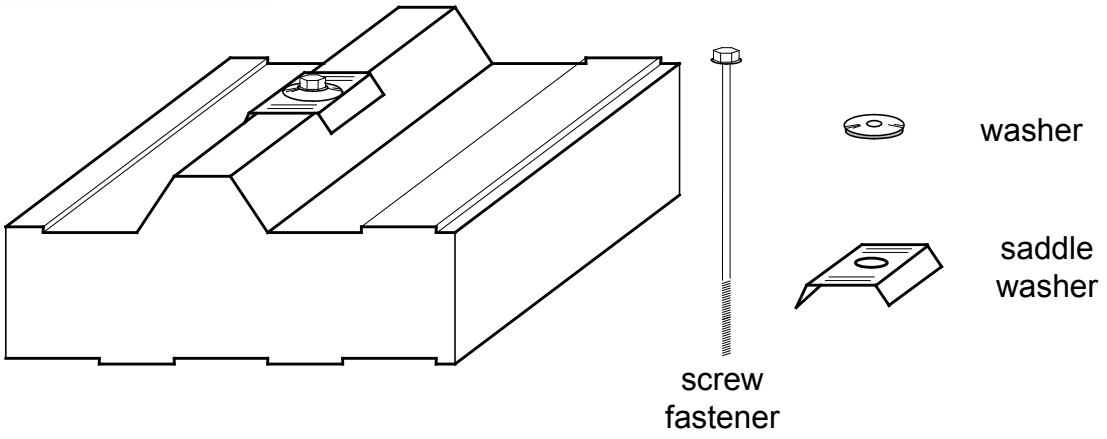

Fig. 32: Saddle washer [7]

The arrangement of the screws was done in combination with double-symmetric I-beams either as alternating fastening or as one-sided fastening. For detailed information about the arrangement of the screws including distances to the edges and between fasteners see report D3.2 – part 1.

5.4 Test set-up

The test set-up for performing tests on torsional bedding was designed following [3] and [5]. The set-up is outlined in Fig. 33 and Fig. 34.

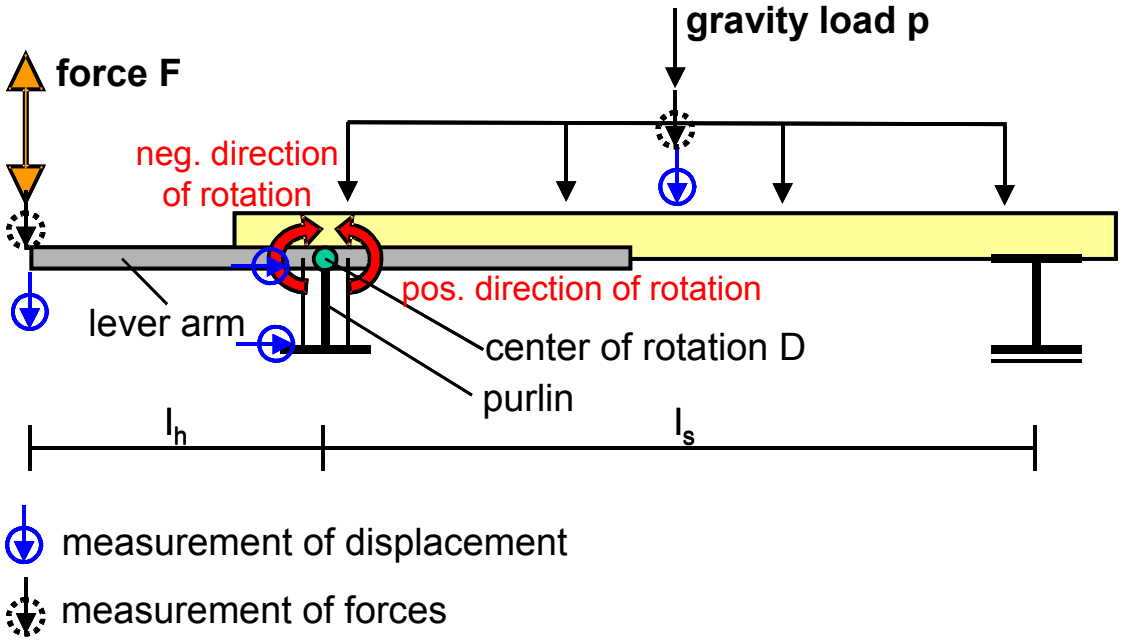

Fig. 33: Test set-up for downward loading

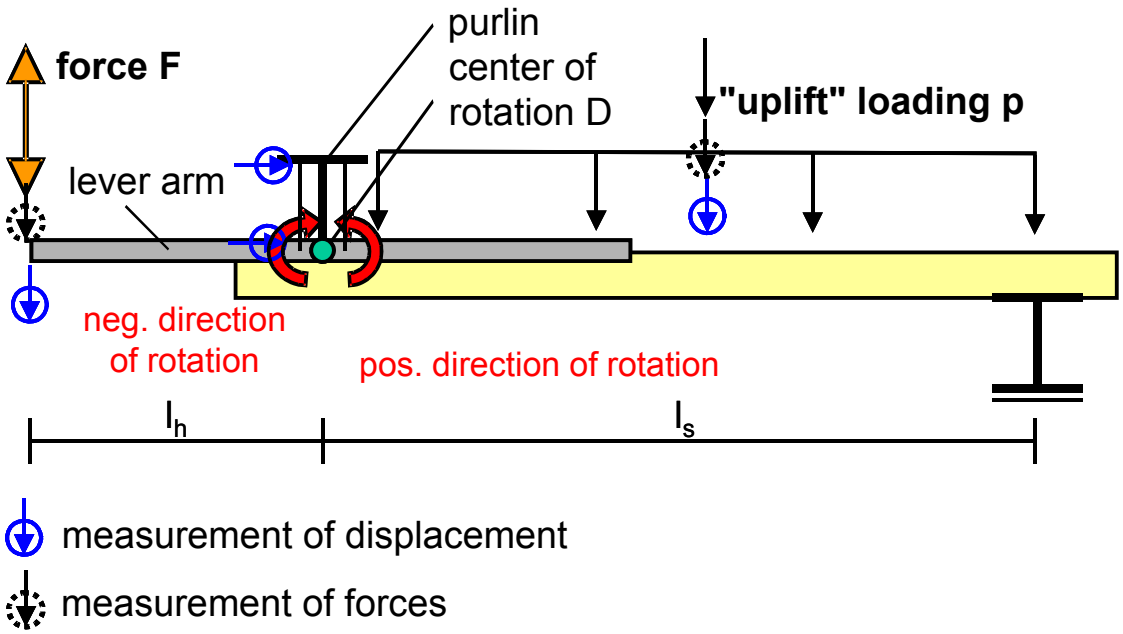

Fig. 34: Test set-up for uplift loading

The test set-up consists of a beam pivoted through a roller bearing, being covered and bolt together as an edge beam of a span with two adjacent sandwich elements, each of width 1 m. The sandwich elements are preloaded through a constant load p_1 during test performance.

At the ends of the beam welded end plates are located, preventing a warping of the beam during test performance. Lever arms are attached rectangular to the longitudinal axis of the beam via these end plates, by means of which the beam can be twisted around the centre of rotation D at simultaneous loading of the sandwich elements according to Fig. 33 and Fig. 34. The lever arms are connected to each other through a transverse truss. The deflection of this system is done through a course controlled hydraulic cylinder loading the transverse truss with the deflection load F. Using roller bearings as well as slide bearings on the second point of support of the sandwich elements it was ensured that neither restraints nor resistances against twisting of the beam occurred from the test set-up.

The displacements v_o and v_u of the upper flange and bottom flange resulting from the rotation of the beam are measured using two cable extension transducers and converted in an appropriate torsion using equation (8).

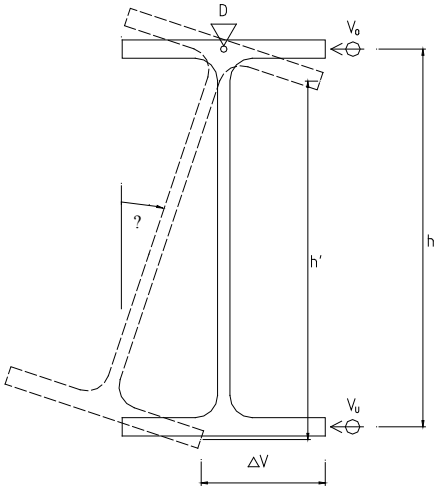

Fig. 35: Centre of rotation D and displacement v_o and v_u

$$\vartheta_M = \arctan\left(\frac{\Delta v_u - \Delta v_o}{h'}\right) = \arcsin\left(\frac{\Delta v_u - \Delta v_o}{h}\right) \qquad \textbf{(26)}$$

5.5 Test performance

After applying a distributed load p_1 to the sandwich elements, the pivoted beam is deflected by means of lever arms. The deflection is done in several cycles alternating in positive and negative torsion direction, where the amplitude of the deflection increases constantly up to a maximum torsions of ϑ = 0,1 rad. After having reached the maximum torsion of ϑ = 0,1 rad in positive as well as in negative torsion direction, an increase of the distributed load occurs whereas the beam is in a non-deflected position. After reaching a load p_2, the torsion of the beam is again applied in cyclic loading. Finally, the torsion of the beam is affected under the load p_3. The value of the load p_3 is always in the limit range of the load-bearing capacity of the sandwich panel. Through this method, the influence of an increased load p on the effect of torsional restraint of the sandwich element can be assessed.

The applied torsional moment as well as the resulting torsion of the beam are recorded continuously and presented as moment-torsion-relation using fully electronic measuring equipment.

A detailed compilation of the tests results can be found in report D3.2 – part 1.

5.6 Evaluation of tests

For each test, the rotational stiffnesses $c_{\vartheta 1}$ and $c_{\vartheta 2}$ were calculated according to [3].

No.	Application	p	$c_{\vartheta 1}$	$c_{\vartheta 1}$	$c_{\vartheta 2}$	$c_{\vartheta 2}$
		[kN/m²]	[kNm/m]			
01	wall	1,30	5,17	4,72	0,37	1,82
		2,09	4,23	4,61	0,44	2,38
		2,87	6,28	6,59	0,40	2,26
02	wall	0,74	2,38	2,18	0,45	1,27
		1,10	2,92	2,91	0,47	1,09
		1,49	3,52	3,26	0,39	1,24
03	wall	1,15	3,48	3,38	0,38	1,35
		1,83	3,61	3,33	0,55	1,66
		2,54	4,60	4,43	0,53	1,63
04a	roof	1,50	2,75	3,36	0,65	1,03
		2,30	3,78	4,07	0,68	1,43
		2,96	4,64	4,75	0,53	1,36
04b	roof	1,50	3,65	4,49	0,83	2,36
		2,30	3,82	4,58	0,89	3,18
		2,96	4,83	4,92	0,83	3,09
05	roof	0,94	17,91	19,01	1,04	4,15
		1,53	15,63	15,79	0,74	4,07
		2,13	18,21	16,39	0,72	3,39
06	wall	1,50	15,40	15,95	0,95	4,15
		2,43	14,90	16,76	0,79	5,25
		3,37	17,77	15,68	0,61	4,87

Tab. 20: $c_{\vartheta 1}$ and $c_{\vartheta 2}$ derived from the tests with downward loading – standard applications

No.	Application	p	$c_{\vartheta 1}$	$c_{\vartheta 1}$	$c_{\vartheta 2}$	$c_{\vartheta 2}$
		[kN/m²]	[kNm/m]			
16	roof	1,07	2,97	2,84	0,329	0,915
		1,50	3,05	2,89	0,313	1,32
		2,06	3,83	3,67	0,35	1,28
16k	roof	1,07	3,66	3,42	0,316	1,13
		1,50	3,62	3,75	0,36	1,845
		2,06	4,51	4,61	0,329	1,76
17	roof	6,1	2,48	2,63	0,37	1,71
		10,9	3,24	3,55	0,389	1,96
		15,0	-	4,95	-	-

Tab. 21: $c_{\vartheta 1}$ and $c_{\vartheta 2}$ derived from the tests with downward loading – roof panels with fixing in the upper flange

Some special remarks have to be given for the tests under uplift loading: Under uplift loading, the relation between the applied rotation and the measured moment different from the one measured under downward loading. Fig. 36 shows schematic the characteristic relation for p = p_1 with p_1 representing the relatively low distributed load at the first load step (see chapter 5.5). In this case fixing only on one side of the flange is assumed. Special notice should be taken to the reloading process in the “strong” direction. During reloading, the measured stiffness is apparently higher (see No. 2 in Fig. 36) than at the time of the first loading (see No. 1 in Fig. 36), but is reduced to the smaller value after exceeding the previous peak value.

Fig. 37 shows the characteristic relation for p > p_1, where $c_{\vartheta 1}$ applies over a wide range of values of ϑ. Finally, an increase to $c_{\vartheta 2}$ in stiffness can be found in the strong direction. For both characteristic relations, the definitions of $c_{\vartheta 1}$ and $c_{\vartheta 2}$ are drawn in.

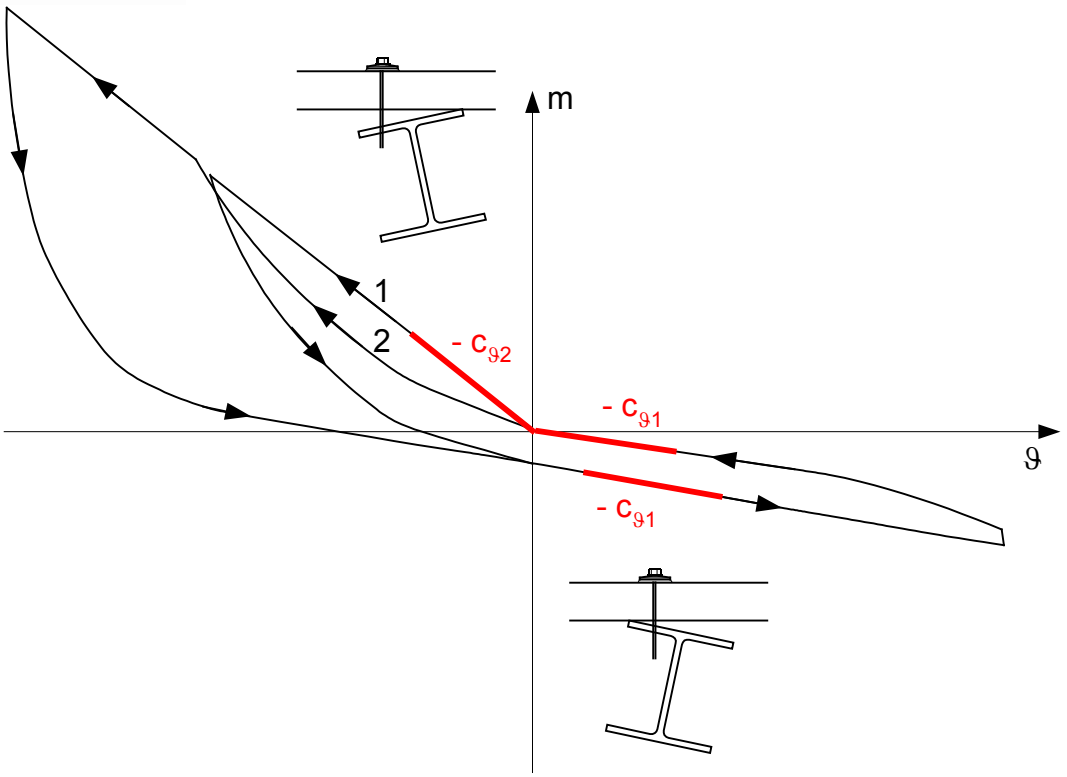

Fig. 36: moment-rotation relation for $p = p_1$

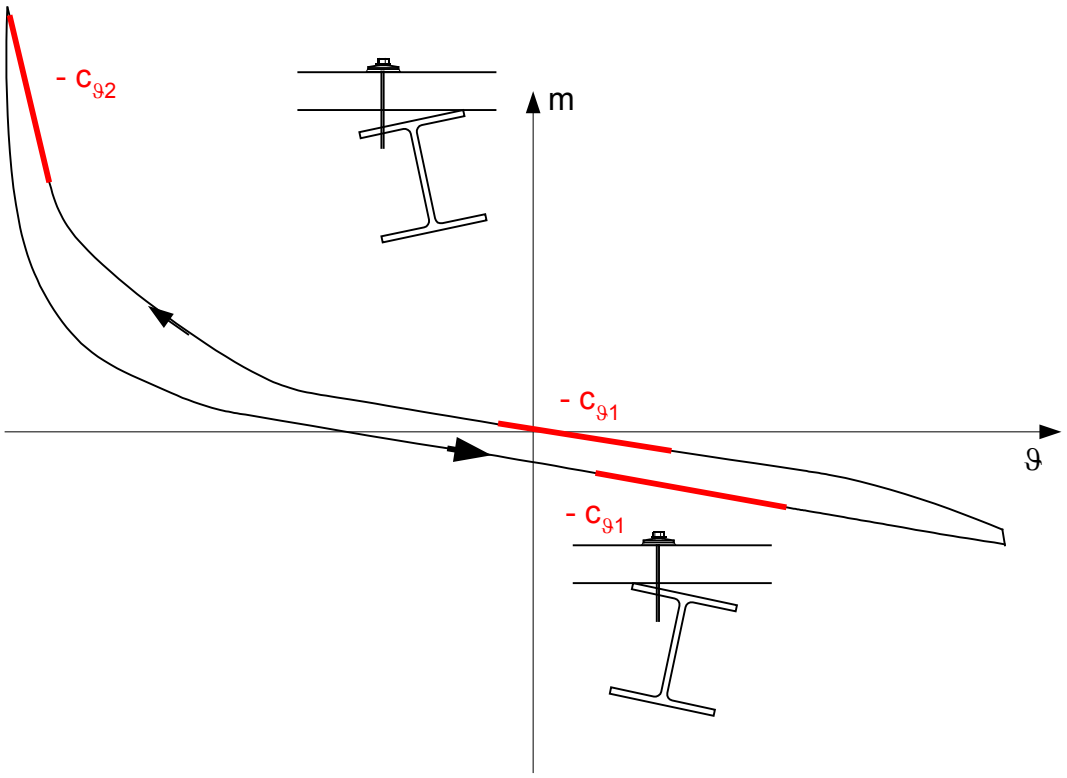

Fig. 37: moment-rotation relation for $p > p_1$

No.	Application	p	$c_{\vartheta 1}$	$c_{\vartheta 1}$	$c_{\vartheta 2}$	$c_{\vartheta 2}$
		[kN/m²]	[kNm/m]			
07	wall	0,92	0,16	-	-	1,37
		1,85	0,14	0,19	-	0,75
		2,31	0,15	0,18	-	0,71
08	wall	0,93	0,10	-	-	7,81
09	wall	0,87	0,31	-	-	3,82
		1,42	0,27	0,33	-	6,96
		1,97	0,26	0,30	-	7,17
10	wall	0,87	0,63	0,67	2,88	2,06
		1,42	0,64	0,74	2,79	1,60
		1,97	0,71	0,72	-	1,24
11	wall	1,25	0,19	0,14	-	1,67
		2,03	0,18	0,23	-	1,76
		2,81	0,16	0,21	-	0,98
12	roof	0,88	0,15	0,22	-	1,91
		1,46	0,14	0,14	-	2,80
		2,02	0,22	0,14	-	2,98
13	roof	0,88	0,19	0,17	-	6,70
		1,46	0,20	0,16	-	13,72
		2,02	0,21	0,22	-	13,90
14	roof	0,66	0,33	0,31	-	11,47
		1,08	0,40	0,31	-	19,13
		1,49	0,46	0,35	-	19,06

Tab. 22: $c_{\vartheta 1}$ and $c_{\vartheta 2}$ derived from the tests with uplift loading – standard applications

No.	Application	p	$c_{\vartheta 1}$	$c_{\vartheta 1}$	$c_{\vartheta 2}$	$c_{\vartheta 2}$
		[kN/m²]	[kNm/m]			
18k	roof	0,90	0,10	0,19	-	0,98
		1,46	-	0,32	-	-
18ok	roof	0,90	0,07	0,18	-	1,02
		1,46	0,11	0,15	-	-
		2,01	0,08	0,15	-	-
19	roof	0,90	0,20	-	0,376	0,582
		1,46	0,19	0,26	-	0,342
		2,01	0,18	-	-	0,228

Tab. 23: $c_{\vartheta 1}$ and $c_{\vartheta 2}$ derived from the tests with uplift loading – roof panels with fixing in the upper flange

Beside these values, some principle observations and results can be found in the results of these tests:

- Comparing tests No. 4a and 4b allows showing the influence of the number of fasteners. In test No. 4a, there were two fasteners per panel while in test No. 4b there were four. While there not that much effect on $c_{\vartheta 1}$, the value $c_{\vartheta 2}$ was more than doubled in the strong direction. This approves the linear dependence of $c_{\vartheta 2}$ with n.
- Comparing tests No. 7 and 8 or 12 and 13 allows showing the influence of the width b of the beams. Increasing the width by a factor of two (IPE160 with a width of 82 mm to an HE160B with a width of 160 mm) leads to an increase of $c_{\vartheta 2}$ by a factor of 3,5 to 4,9, means approx. 2^2. This approves the quadratic dependency of $c_{\vartheta 2}$ with b.
- Comparing tests No. 9 and 10 allows showing the influence of the fixing pattern. Both tests were performed with the same number of fasteners, but different pattern. While in test No. 9, there is a weak direction; test No. 10 shows comparable values of $c_{\vartheta 2}$ in both directions. Due to the fact that half of the fasteners have a smaller lever arm, the value is smaller than the one obtained in test No. 9.
- Comparing tests No. 16 and 16k or 18 and 18k allows showing the influence of a saddle washer. While there is a slight increase in stiffness when using a saddle washer, the increase is not that high to be used for design purposes.

5.7 Material properties

After test performance, specimens for tensile tests according to DIN EN 10002-1 were worked out from the slightly stressed ranges of upper and lower surface layer at each tested type of element with metallic faces. For GFRP faces specimens for tensile tests according to DIN EN

ISO 527-4 were worked out from samples taken from the batches used for the tests on torsional restraint.

The performance of tensile tests for determining the mechanical properties of surface layers was done on a universal testing machine of the Versuchsanstalt für Stahl, Holz und Steine of Karlsruhe Institute of Technology.

For the determination of the yield strength $R_{eH}/R_{p0,2}$ and the tensile strength $R_{m,}$ the core thicknesses determined on the specimens were used.

In addition, tension/compression tests with a test device according to Gehring [6] were performed on GFRP facings for determining the modulus under compression and tensile loading. The mechanical properties were determined according to [N3]. The determination of the compression strength f_{Cc} β_z, the tensile strength f_{Ct}, the shear strength f_{Cv}, the density ρ, as well as the appropriate shear, compression and tensile module values G_C, E_{Cc} and E_{Ct} was realized on at least three specimens. For the compression and tensile tests, specimens with the dimension 100 m 100 x thickness of the element were taken from panels not used for the tests on torsional restraint. The analysis of the modulus of elasticity E_C was realised as mean value from the compression and tensile module of a specimen pair.

6 Determination of the torsional spring stiffnesses $c_{\vartheta 1}$ and $c_{\vartheta 2}$

6.1 Introduction

From the mechanical model and its discussion the following conclusions can be drawn for the further evaluation:

- Preliminary evaluations showed that no differentiation between EPS and PUR is necessary. Therefore just two groups of core materials have to be distinguished: foam material and mineral wool, each defining one population in following the statistical evaluation.
- The stiffness of the faces has an influence on the torsional restraint. A differentiation between flat or lightly profiled panels on the one hand and strongly profiled faces has to be done. In this case, the evaluation has to be done separately for the different applications “wall” and “roof” or “flat or lightly profiled panels” and “profiled panels”, respectively. Each population has to be divided into these sub-populations.
- At least theoretical, there is no influence of the elastic modulus of the face material E_F. In fact, a difference in results for metallic faces and faces made of GFRP was found. A reduction factor for GFRP faces will be introduced.
- No distinction will be made between applications with and without saddle washers.
- For wind suction/uplift loading, $c_{\vartheta 1} = c_{\vartheta 2} = 0$ has to be assumed.

- The values $c_{\vartheta 2}$ obtained for low uplift forces will be used in evaluation: Using the described mechanical models, the stiffnesses $c_{\vartheta 2}$ for both downward and uplift loading can be evaluated together. For this value, the number of fasteners and their arrangement has to be taken into account.

The torsional stiffness was evaluated using all available test data: The tests of Dürr [3] were included in the evaluation:

1. All panels define a population. This population has sub-populations because of the different core materials ("foam material" and "mineral wool") and different applications and corresponding geometry of the outer face ("flat or lightly profiled panels" and "profiled panels"). There are four sub-populations in total. Other definitions of populations were checked, but did not lead to that different results, see, for example, [4].
2. Based on the test results $c_{\vartheta 1,test}$ and $c_{\vartheta 2,test}$, the numerical parameters c_1 and c_2, respectively, were calculated for each test and the mean values $c_{1,mean}$ and $c_{\vartheta 2,mean}$ were calculated for each sub-population.
3. A statistical evaluation according to EN 1990, Annex D, was performed, using a Gaussian (normal) distribution. For each test, the values $c_{\vartheta 1}$ or $c_{\vartheta 2}$ were calculated based on $c_{\vartheta 1,calc}$ and $c_{\vartheta 2,calc}$. The ratios $c_{\vartheta 1,calc}/c_{\vartheta 1,test}$ and $c_{\vartheta 2,calc}/c_{\vartheta 2,test}$ were calculated for each test with the corresponding vales of $c_{\vartheta 1,calc}$ or $c_{\vartheta 2,calc,}$ respectively.
4. The standard deviations s_1 and s_2 of these ratios was calculated for c_1 and c_2 separately.
5. The characteristic values were calculated with

$$c_{1,k} = c_1 = c_{1,mean} \cdot \left(1 - k_n \cdot s_1\right) \quad \textbf{(27)}$$

and

$$c_{2,k} = c_2 = c_{1,mean} \cdot \left(1 - k_n \cdot s_2\right) \quad \textbf{(28)}$$

for each sub-population, using k_n according to DIN 1990, Annex D

6. The reduction factors $c_{F,1}$ and $c_{F,2}$ for GFRP-faces was calculated to obtain the best fit with the other data. The smallest value of $c_{F,1}$ and $c_{F,2}$ applies.

The calculation model is valid in the investigated application range. This application range is given in the appendix.

6.2 Determination of $c_{\vartheta 1}$

For the determination of $c_{\vartheta 1}$ under downward loading the approach

$$c_{\vartheta 1} = c_1 \cdot b^2 \cdot E_C \quad \textbf{(29)}$$

was used. The following table lists all of the results evaluated from our tests as well as from [3]. The width b of the adjacent flange and the material properties are listed as well.

source		$c_{\vartheta 1,test}$	E_F	E_C	b	c_1	$c_{\vartheta 1,calc}$	ratio
		Nm/m	N/mm²	N/mm²	mm	10^{-4}	Nm/m	-
flat or lightly profiled, PU core, values acc. to [3]		5292	210000	4,1	82	0,192	5757	0,919
		6237	210000	4,1	82	0,226	5757	1,083
		6480	210000	4,1	82	0,235	5757	1,126
		4788	210000	4,1	82	0,174	5757	0,832
		6273	210000	4,1	82	0,228	5757	1,090
		6687	210000	4,1	82	0,243	5757	1,161
		5814	210000	4,1	82	0,211	5757	1,010
		6669	210000	4,1	82	0,242	5757	1,158
		6714	210000	4,1	82	0,244	5757	1,166
		4401	210000	3,5	82	0,187	4915	0,895
		4410	210000	3,5	82	0,187	4915	0,897
		4446	210000	3,5	82	0,189	4915	0,905
		4410	210000	3,5	82	0,187	4915	0,897
		5814	210000	3,5	82	0,247	4915	1,183
		5490	210000	4,0	82	0,204	5617	0,977
		5859	210000	4,0	82	0,218	5617	1,043
		5292	210000	4,0	82	0,197	5617	0,942
		5508	210000	4,1	82	0,200	5757	0,957
		6633	210000	4,1	82	0,241	5757	1,152
		6921	210000	4,1	82	0,251	5757	1,202
		5553	210000	4,1	82	0,201	5757	0,965
		6246	210000	4,1	82	0,227	5757	1,085
		6687	210000	4,1	82	0,243	5757	1,161
		6975	210000	4,1	82	0,253	5757	1,212
		6912	210000	4,1	82	0,251	5757	1,201
		6948	210000	4,1	82	0,252	5757	1,207
		4761	210000	3,5	82	0,202	4915	0,969
		4572	210000	3,5	82	0,194	4915	0,930
		4698	210000	3,5	82	0,200	4915	0,956
		4617	210000	3,5	82	0,196	4915	0,939
		6354	210000	3,5	82	0,270	4915	1,293
		6867	210000	4,0	82	0,255	5617	1,223
		6219	210000	4,0	82	0,231	5617	1,107
		5508	210000	4,0	82	0,205	5617	0,981
flat or lightly profiled, PU core, values acc. to D3.2 – part 1	1	5170	210000	4,14	82	0,170	6361	0,813
	1	4230	210000	4,14	82	0,139	6361	0,665
	1	6280	210000	4,14	82	0,206	6361	0,987
	1	4720	210000	4,14	82	0,155	6361	0,742
	1	4610	210000	4,14	82	0,151	6361	0,725
	1	6590	210000	4,14	82	0,216	6361	1,036
	2	2380	7000	3,25	82	0,173	2877	0,827
	2	2924	7000	3,25	82	0,212	2877	1,016
	2	3520	7000	3,25	82	0,256	2877	1,224
	2	2180	7000	3,25	82	0,158	2877	0,758
	2	2910	7000	3,25	82	0,211	2877	1,012
	2	3260	7000	3,25	82	0,237	2877	1,133
	3	3480	70000	2,37	82	0,173	4199	0,829
	3	3610	70000	2,37	82	0,180	4199	0,860
	3	4600	70000	2,37	82	0,229	4199	1,096
	3	3380	70000	2,37	82	0,168	4199	0,805
	3	3330	70000	2,37	82	0,166	4199	0,793
	3	4427	70000	2,37	82	0,220	4199	1,054

Tab. 24: Determination of c_1 – part 1

source		$c_{\vartheta 1,test}$	E_F	E_C	b	c_1	$c_{\vartheta 1,calc}$	ratio
		Nm/m	N/mm²	N/mm²	mm	10^{-4}	Nm/m	-
flat or lightly profiled, PU core	6	15400	210000	3,03	160	0,193	16627	0,926
	6	14900	210000	3,03	160	0,187	16627	0,896
	6	17770	210000	3,03	160	0,223	16627	1,069
	6	15950	210000	3,03	160	0,200	16627	0,959
	6	16760	210000	3,03	160	0,211	16627	1,008
	6	15680	210000	3,03	160	0,197	16627	0,943
profiled, PU core, values acc. to [3]		5553	210000	3,9	82	0,212	6939	0,800
		8226	210000	3,9	82	0,314	6939	1,185
		7830	210000	3,9	82	0,299	6939	1,128
		7497	210000	4,5	82	0,248	8006	0,936
		7992	210000	4,5	82	0,264	8006	0,998
		7893	210000	4,5	82	0,261	8006	0,986
		8694	210000	3,9	82	0,332	6939	1,253
		5418	210000	3,9	82	0,207	6939	0,781
		9180	210000	3,9	82	0,350	6939	1,323
		8253	210000	3,9	82	0,315	6939	1,189
		7623	210000	3,9	82	0,291	6939	1,099
		8550	210000	3,9	82	0,326	6939	1,232
		5310	210000	4,5	82	0,175	8006	0,663
		7650	210000	4,5	82	0,253	8006	0,955
		8550	210000	4,5	82	0,283	8006	1,068
		6030	210000	3,9	82	0,230	6939	0,869
		7650	210000	3,9	82	0,292	6939	1,102
		8190	210000	3,9	82	0,312	6939	1,180
		6453	210000	3,9	82	0,246	6939	0,930
		7785	210000	3,9	82	0,297	6939	1,122
		8541	210000	3,9	82	0,326	6939	1,231
		5886	210000	3,9	82	0,224	6939	0,848
		8298	210000	3,9	82	0,316	6939	1,196
		8253	210000	3,9	82	0,315	6939	1,189
		10629	210000	4,5	82	0,351	8006	1,328
		9630	210000	4,5	82	0,318	8006	1,203
		9378	210000	4,5	82	0,310	8006	1,171
		10287	210000	3,9	82	0,392	6939	1,483
		6084	210000	3,9	82	0,232	6939	0,877
		9072	210000	3,9	82	0,346	6939	1,307
		7623	210000	3,9	82	0,291	6939	1,099
		7785	210000	3,9	82	0,297	6939	1,122
		8910	210000	3,9	82	0,340	6939	1,284
		5670	210000	4,5	82	0,187	8006	0,708
		8640	210000	4,5	82	0,286	8006	1,079
		9810	210000	4,5	82	0,324	8006	1,225
		8190	210000	3,9	82	0,312	6939	1,180
		9540	210000	3,9	82	0,364	6939	1,375
		9180	210000	3,9	82	0,350	6939	1,323
		6750	210000	3,9	82	0,257	6939	0,973
		8055	210000	3,9	82	0,307	6939	1,161
		8901	210000	3,9	82	0,339	6939	1,283

Tab. 25: Determination of c_1 – part 2

source		$c_{\vartheta 1,test}$	E_F	E_C	b	c_1	$c_{\vartheta 1,calc}$	ratio
		Nm/m	N/mm²	N/mm²	mm	10^{-4}	Nm/m	-
profiled, PU core, values acc. to D3.2 – part 1	04a	2750	70000	2,7	82	0,151	4804	0,572
	04a	3780	70000	2,7	82	0,208	4804	0,787
	04a	4640	70000	2,7	82	0,256	4804	0,966
	04a	3360	70000	2,7	82	0,185	4804	0,699
	04a	4071	70000	2,7	82	0,224	4804	0,847
	04a	4750	70000	2,7	82	0,262	4804	0,989
	04b	3646	70000	2,7	82	0,201	4804	0,759
	04b	3820	70000	2,7	82	0,210	4804	0,795
	04b	4830	70000	2,7	82	0,266	4804	1,005
	04b	4490	70000	2,7	82	0,247	4804	0,935
	04b	4580	70000	2,7	82	0,252	4804	0,953
	04b	4920	70000	2,7	82	0,271	4804	1,024
	16	2970	210000	2,61	82	0,169	4644	0,640
	16	3050	210000	2,61	82	0,174	4644	0,657
	16	3830	210000	2,61	82	0,218	4644	0,825
	16	2840	210000	2,61	82	0,162	4644	0,612
	16	2890	210000	2,61	82	0,165	4644	0,622
	16	3670	210000	2,61	82	0,209	4644	0,790
	16k	3660	210000	2,61	82	0,209	4644	0,788
	16k	3620	210000	2,61	82	0,206	4644	0,780
	16k	4510	210000	2,61	82	0,257	4644	0,971
	16k	3420	210000	2,61	82	0,195	4644	0,736
	16k	3750	210000	2,61	82	0,214	4644	0,808
	16k	4610	210000	2,61	82	0,263	4644	0,993
flat or lightly profiled, MW core, values acc. to [3]		4050	210000	8,9	82	0,068	4220	0,960
		4095	210000	8,9	82	0,068	4220	0,970
		4194	210000	8,9	82	0,070	4220	0,994
		3960	210000	8,9	82	0,066	4220	0,938
		4518	210000	8,9	82	0,075	4220	1,071
		4500	210000	8,9	82	0,075	4220	1,066
profiled, MW core, values acc. to [3]		4653	210000	6,9	82	0,100	6064	0,767
		4500	210000	6,9	82	0,097	6064	0,742
		4770	210000	6,9	82	0,103	6064	0,787
		4887	210000	6,9	82	0,105	6064	0,806
		4689	210000	6,9	82	0,101	6064	0,773
		5004	210000	6,9	82	0,108	6064	0,825
profiled, MW core, values acc. to D3.2 – part 1	5	17910	210000	4,06	160	0,172	13585	1,318
	5	15630	210000	4,06	160	0,150	13585	1,151
	5	18210	210000	4,06	160	0,175	13585	1,340
	5	19010	210000	4,06	160	0,183	13585	1,399
	5	15790	210000	4,06	160	0,152	13585	1,162
	5	16390	210000	4,06	160	0,158	13585	1,206
	17	2480	210000	4,06	82	0,091	3568	0,695
	17	3240	210000	4,06	82	0,119	3568	0,908
	17	2630	210000	4,06	82	0,096	3568	0,737
	17	3550	210000	4,06	82	0,130	3568	0,995
	17	4950	210000	4,06	82	0,181	3568	1,387

Tab. 26: Determination of c_1 – part 2

Core material	geometry of outer face (at the head of fasteners)	$c_{1,mean}$	$c_{1,k}$
PUR/EPS	profiled	0,265	0,180
	lightly profiled/flat	0,209	0,142
Mineral wool	profiled	0,131	0,089
	lightly profiled/flat	0,071	0,048

Tab. 27: Results of statistical evaluation

The statistical parameters were:

- standard deviation s_1 = 0,189
- variance 18,9%
- number of results n = 147
- k-factor k_n = 1,68

The value of the spring stiffness for mineral wool is approximately 30% to 50% of the value for the foamed core materials PUR and EPS. The reason for this can be found in the lower shear stiffness and lower ratio shear stiffness/elastic modulus. The influence of the stiffness of the faces was investigated, too: From the statistical evaluation an additional reduction factor of c_F = 0,43 for faces made of GFRP was obtained. The thickness of GFRP faces has to be in the range of 1,70 mm to 2,00 mm. No reduction factor for aluminium faces is required.

Finally we obtain

$$c_{\vartheta 1,mean} = c_{1,mean} \cdot c_F \cdot b^2 \cdot E_C \qquad \textbf{(30)}$$

and

$$c_{\vartheta 1,k} = c_{1,k} \cdot c_F \cdot b^2 \cdot E_C \qquad \textbf{(31)}$$

The mean value $c_{1,mean}$ can be compared with the theoretically determined value from chapter 3: Equation (16) gives c_1 = 0,222 for ν_C = 0,0 and c_1 = 0,199 for ν_C = 0,3. Differences result from the scatter in test results and the assumptions in material properties and mechanical model. For design purposes, the test results given in Tab. 27 should be used, because they cover the scatter in parameters and (especially for mineral wool) they represent the actual material properties and material behaviour.

Due to the different mechanical model, the numerical parameters deviate from the ones given in [3] by order of approximately 10.

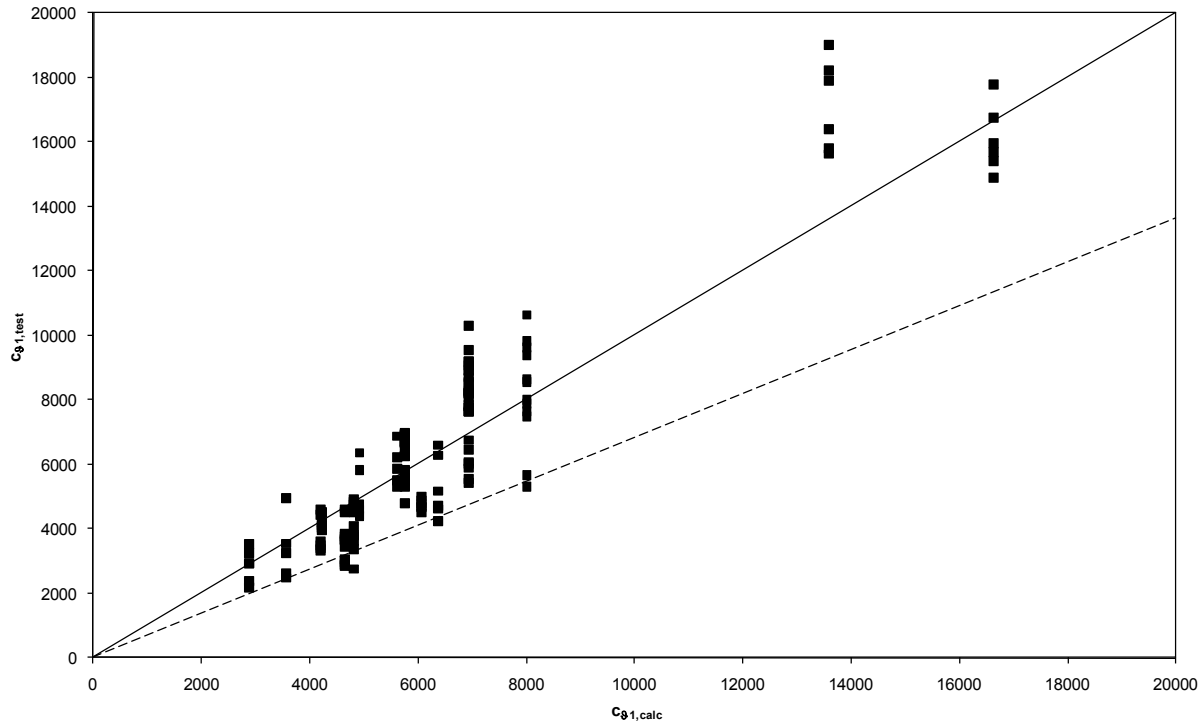

Fig. 38: Comparison of tests results with calculated values

6.3 Determination of $c_{\vartheta 2}$

For the determination of $c_{\vartheta 2}$ under downward the approach

$$c_{\vartheta 2} = c_2 \cdot n \cdot b_k^2 \cdot E_C \qquad \textbf{(32)}$$

was used. The parameter b instead of b_K is used for the lever arm between the contact line at the edge of the flange and the location of the fasteners.

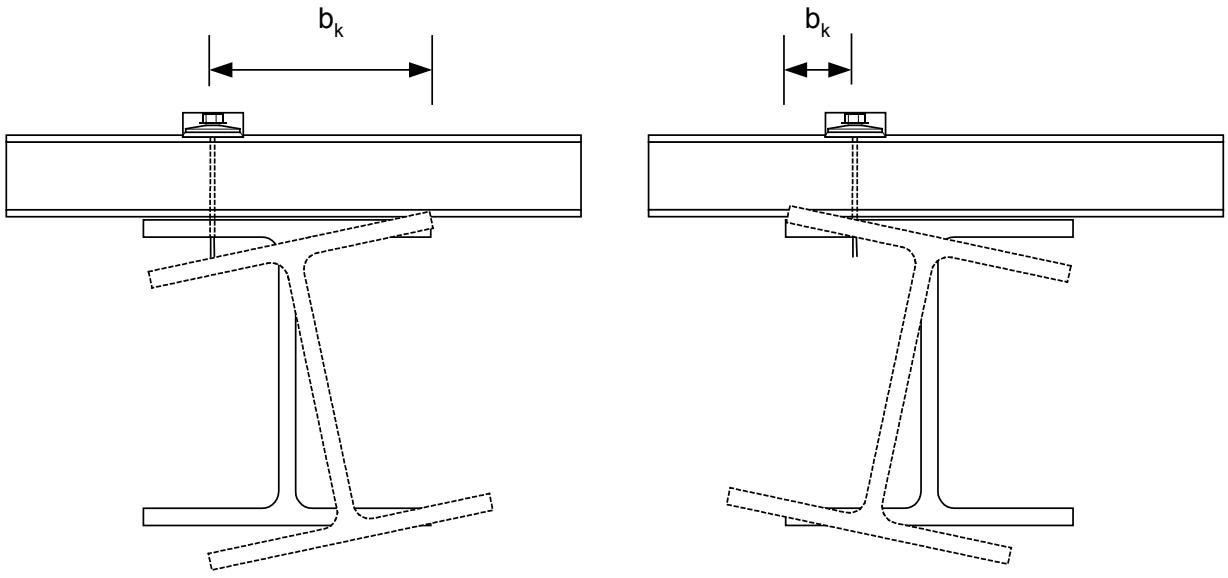

Fig. 39: Lever arm b_K

The additional factor n takes account for the number of fasteners per unit length. For alternating fixing patterns only the number of fasteners with the biggest lever arm b_k should be taken into account.

For evaluation the following applies:

- Both uplift and downward loading was included.
- For $b_K \approx 0{,}25 \cdot b$ a big scatter in results was obtained because of the low absolute values. These values were not included in the statistical evaluation. Nevertheless recalculation showed a quite good agreement with the between values.
- No differentiation between the fixing points was to be done for panels with strongly profiled faces, where fixing is possible in the lower flange or in the upper flange.

The following table lists all of the results evaluated from our tests as well as from [3].

source	$c_{\vartheta 2,test}$	E_F	E_C	b_K	n	c_2	$c_{\vartheta 2,calc}$	ratio
	Nm/m	N/mm²	N/mm²	mm	m^{-1}	m	Nm/m	-
flat or lightly profiled, PU core, values acc. to [3]	756	210000	4,1	61,5	1	0,049	1057	0,715
	891	210000	4,1	61,5	1	0,057	1057	0,843
	864	210000	4,1	61,5	1	0,056	1057	0,818
	1134	210000	4,1	61,5	1	0,073	1057	1,073
	1170	210000	4,1	61,5	1	0,075	1057	1,107
	1044	210000	4,1	61,5	1	0,067	1057	0,988
	531	210000	4,1	20,5	2	-	235	-
	405	210000	4,1	20,5	2	-	235	-
	396	210000	4,1	20,5	2	-	235	-
	1053	210000	3,5	61,5	1	0,080	902	1,167
	1260	210000	3,5	61,5	1	0,095	902	1,397
	1107	210000	3,5	61,5	1	0,084	902	1,227
	1224	210000	3,5	61,5	1	0,092	902	1,357
	1152	210000	3,5	61,5	1	0,087	902	1,277
	1179	210000	4,0	61,5	1	0,078	1031	1,144
	1188	210000	4,0	61,5	1	0,079	1031	1,152
	954	210000	4,1	61,5	1	0,062	1057	0,903
	918	210000	4,1	61,5	1	0,059	1057	0,869
	855	210000	4,1	61,5	1	0,055	1057	0,809
	1026	210000	4,1	61,5	1	0,066	1057	0,971
	1287	210000	4,1	61,5	1	0,083	1057	1,218
	1224	210000	4,1	61,5	1	0,079	1057	1,158
	1845	210000	4,1	61,5	2	0,059	2113	0,873
	2097	210000	4,1	61,5	2	0,068	2113	0,992
	2322	210000	4,1	61,5	2	0,075	2113	1,099
	954	210000	3,5	61,5	1	0,072	902	1,058
	1260	210000	3,5	61,5	1	0,095	902	1,397
	981	210000	3,5	61,5	1	0,074	902	1,087
	1269	210000	3,5	61,5	1	0,096	902	1,407
	1323	210000	3,5	61,5	1	0,100	902	1,467
	855	210000	4,0	61,5	1	0,057	1031	0,829
	846	210000	4,0	61,5	1	0,056	1031	0,821

Tab. 28: Determination of c_2 – part 1

source		$c_{\vartheta 2,test}$	E_F	E_C	b_K	n	c_2	$c_{\vartheta 2,calc}$	ratio
		Nm/m	N/mm²	N/mm²	mm	m^{-1}	m	Nm/m	-
flat or lightly profiled, PU core, values acc. to D3.2 – part 1	1	370	210000	4,53	20,5	2	-	259	-
	1	400	210000	4,53	20,5	2	-	259	-
	1	400	210000	4,53	20,5	2	-	259	-
	1	1820	210000	4,53	61,5	2	0,053	2335	0,779
	1	2380	210000	4,53	61,5	2	0,069	2335	1,019
	1	2260	210000	4,53	61,5	2	0,066	2335	0,968
	2	450	7000	4,78	20,5	2	-	127	-
	2	470	7000	4,78	20,5	2	-	127	-
	2	390	7000	4,78	20,5	2	-	127	-
	2	1270	7000	4,78	61,5	2	0,076	1144	1,110
	2	1090	7000	4,78	61,5	2	0,065	1144	0,953
	2	1240	7000	4,78	61,5	2	0,074	1144	1,084
	3	379	70000	2,99	20,5	2	-	171	-
	3	550	70000	2,99	20,5	2	-	171	-
	3	530	70000	2,99	20,5	2	-	171	-
	3	1350	70000	2,99	61,5	2	0,060	1541	0,876
	3	1660	70000	2,99	61,5	2	0,073	1541	1,077
	3	1630	70000	2,99	61,5	2	0,072	1541	1,058
	6	947	210000	3,11	40	2	-	678	-
	6	791	210000	3,11	40	2	-	678	-
	6	610	210000	3,11	40	2	-	678	-
	6	4150	210000	3,11	120	2	0,046	6103	0,680
	6	5250	210000	3,11	120	2	0,059	6103	0,860
	6	4870	210000	3,11	120	2	0,054	6103	0,798
	7	1370	210000	3,11	61,5	2	0,058	1603	0,855
	7	750	210000	3,11	61,5	2	0,032	1603	0,468
	7	713	210000	3,11	61,5	2	0,030	1603	0,445
	8	7810	210000	3,11	120	2	0,087	6103	1,280
	11	1670	210000	4,53	61,5	2	0,049	2335	0,715
	11	1760	210000	4,53	61,5	2	0,051	2335	0,754
profiled, PU core, values acc. to [3]		1413	210000	3,9	61,5	1	0,096	1005	1,079
		1269	210000	3,9	61,5	1	0,086	1005	0,969
		1287	210000	3,9	61,5	1	0,087	1005	0,983
		1683	210000	4,5	61,5	1	0,099	1160	1,114
		1836	210000	4,5	61,5	1	0,108	1160	1,215
		1800	210000	4,5	61,5	1	0,106	1160	1,191
		1962	210000	3,9	61,5	2	0,067	2010	0,749
		2070	210000	3,9	61,5	2	0,070	2010	0,790
		1980	210000	3,9	61,5	2	0,067	2010	0,756
		1476	210000	3,9	61,5	1	0,100	1005	1,127
		1530	210000	3,9	61,5	1	0,104	1005	1,168
		1485	210000	3,9	61,5	1	0,101	1005	1,134
		1845	210000	4,5	61,5	1	0,108	1160	1,221
		1953	210000	4,5	61,5	1	0,115	1160	1,292
		1998	210000	4,5	61,5	1	0,117	1160	1,322

Tab. 29: Determination of c_2 – part 2

source		$c_{\vartheta 2,test}$	E_F	E_C	b_K	n	c_2	$c_{\vartheta 2,calc}$	ratio
		Nm/m	N/mm²	N/mm²	mm	m^{-1}	m	Nm/m	-
profiled, PU core, values acc. to [3]		1872	210000	3,9	61,5	1	0,127	1005	1,429
		1611	210000	3,9	61,5	1	0,109	1005	1,230
		1260	210000	3,9	61,5	1	0,085	1005	0,962
		1413	210000	3,9	61,5	1	0,096	1005	1,079
		1197	210000	3,9	61,5	1	0,081	1005	0,914
		1215	210000	3,9	61,5	1	0,082	1005	0,928
		1422	210000	4,5	61,5	1	0,084	1160	0,941
		1737	210000	4,5	61,5	2	0,051	2320	0,575
		1611	210000	4,5	61,5	2	0,047	2320	0,533
		2358	210000	3,9	61,5	2	0,080	2010	0,900
		1710	210000	3,9	61,5	1	0,116	1005	1,306
		1800	210000	3,9	61,5	1	0,122	1005	1,374
		1053	210000	3,9	61,5	1	0,071	1005	0,804
		1080	210000	3,9	61,5	1	0,073	1005	0,825
		1062	210000	3,9	61,5	1	0,072	1005	0,811
		1575	210000	4,5	61,5	1	0,093	1160	1,042
		1611	210000	4,5	61,5	1	0,095	1160	1,066
		1431	210000	4,5	61,5	1	0,084	1160	0,947
		1377	210000	3,9	61,5	1	0,093	1005	1,051
		2043	210000	3,9	61,5	1	0,139	1005	1,560
		1917	210000	3,9	61,5	1	0,130	1005	1,464
profiled, PU core, values acc. to D3.2 – part 1	04a	650	70000	2,7	20,5	2	-	155	-
	04a	678	70000	2,7	20,5	2	-	155	-
	04a	526	70000	2,7	20,5	2	-	155	-
	04a	1030	70000	2,7	61,5	2	0,050	1392	0,568
	04a	1429	70000	2,7	61,5	2	0,070	1392	0,788
	04a	1355	70000	2,7	61,5	2	0,066	1392	0,747
	04b	825	70000	2,7	20,5	4	-	309	-
	04b	887	70000	2,7	20,5	4	-	309	-
	04b	833	70000	2,7	20,5	4	-	309	-
	04b	2358	70000	2,7	61,5	4	0,058	2784	0,650
	04b	3180	70000	2,7	61,5	4	0,078	2784	0,877
	04b	3090	70000	2,7	61,5	4	0,076	2784	0,852
	12	1910	210000	2,61	61,5	3	0,064	2018	0,726
	12	2800	210000	2,61	61,5	3	0,095	2018	1,065
	12	2980	210000	2,61	61,5	3	0,101	2018	1,133
	13	6700	210000	2,61	120	3	0,059	7683	0,669
	13	13720	210000	2,61	120	3	0,122	7683	1,370
	13	13900	210000	2,61	120	3	0,123	7683	1,388
	16	329	210000	2,61	20,5	1,5	-	112	-
	16	313	210000	2,61	20,5	1,5	-	112	-
	16	350	210000	2,61	20,5	1,5	-	112	-
	16	915	210000	2,61	61,5	1,5	0,062	1009	0,696
	16	1320	210000	2,61	61,5	1,5	0,089	1009	1,004
	16	1280	210000	2,61	61,5	1,5	0,086	1009	0,974
	16k	316	210000	2,61	20,5	1,5	-	112	-
	16k	360	210000	2,61	20,5	1,5	-	112	-
	16k	329	210000	2,61	20,5	1,5	-	112	-
	16k	1130	210000	2,61	61,5	1,5	0,076	1009	0,859
	16k	1845	210000	2,61	61,5	1,5	0,125	1009	1,403
	16k	1760	210000	2,61	61,5	1,5	0,119	1009	1,339

Tab. 30: Determination of c_2 – part 3

source		$c_{\vartheta 2,test}$	E_F	E_C	b_K	n	c_2	$c_{\vartheta 2,calc}$	ratio
		Nm/m	N/mm²	N/mm²	mm	m^{-1}	m	Nm/m	-
profiled, PU core, D3.2	18k	976	210000	2,61	61,5	1,5	0,066	1009	0,742
	18ok	1019	210000	2,61	61,5	1,5	0,069	1009	0,775
	19	376	210000	2,61	61,5	0,5	0,076	336	0,858
	19	582	210000	2,61	61,5	1	0,059	673	0,664
	19	342	210000	2,61	61,5	1	-	673	-
	19	228	210000	2,61	61,5	1	-	673	-
flat or lightly profiled, MW core, values acc. to [3]		1188	210000	8,9	61,5	1	0,035	1545	0,769
		1278	210000	8,9	61,5	1	0,038	1545	0,827
		1188	210000	8,9	61,5	1	0,035	1545	0,769
		1116	210000	8,9	61,5	1	0,033	1545	0,722
		1692	210000	8,9	61,5	1	0,050	1545	1,095
		1737	210000	8,9	61,5	1	0,052	1545	1,125
flat or lightly profiled, MW core, to D3.2	9	3820	210000	6,72	61,5	4	0,038	4665	0,819
	9	6960	210000	6,72	61,5	4	0,068	4665	1,492
	9	7170	210000	6,72	61,5	4	0,071	4665	1,537
	10	2880	210000	6,72	61,5	2	0,057	2333	1,235
	10	2790	210000	6,72	61,5	2	0,055	2333	1,196
	10	2790	210000	6,72	61,5	2	0,055	2333	1,196
	10	1600	210000	6,72	61,5	2	0,031	2333	0,686
	10	1240	210000	6,72	61,5	2	0,024	2333	0,532
profiled, MW core, values acc. to [3]		954	210000	6,9	61,5	1	0,037	1176	0,811
		1125	210000	6,9	61,5	1	0,043	1176	0,957
		981	210000	6,9	61,5	1	0,038	1176	0,834
		927	210000	6,9	61,5	1	0,036	1176	0,788
		1188	210000	6,9	61,5	1	0,046	1176	1,010
		1044	210000	6,9	61,5	1	0,040	1176	0,888
profiled, MW core, values acc. to D3.2 – part 1	5	1044	210000	4,06	40	2	-	585	-
	5	739	210000	4,06	40	2	-	585	-
	5	720	210000	4,06	40	2	-	585	-
	5	4150	210000	4,06	120	2	0,035	5268	0,788
	5	4070	210000	4,06	120	2	0,035	5268	0,773
	5	3390	210000	4,06	120	2	0,029	5268	0,643
	14	11470	210000	4,06	120	4	0,049	10537	1,089
	14	19130	210000	4,06	120	4	0,082	10537	1,816
	14	19060	210000	4,06	120	4	0,082	10537	1,809
	17	370	210000	4,06	20,5	4	0,054	308	1,203
	17	389	210000	4,06	20,5	4	0,057	308	1,265
	17	1710	210000	4,06	61,5	4	0,028	2768	0,618
	17	1960	210000	4,06	61,5	4	0,032	2768	0,708

Tab. 31: Determination of c_2 – part 4

Core material	geometry of outer face (at the head of fasteners)	$c_{2,mean}$	$c_{2,k}$
PUR/EPS	profiled	0,089 m	0,052 m
	lightly profiled/flat	0,068 m	0,040 m
Mineral wool	profiled	0,045 m	0,027 m
	lightly profiled/flat	0,046 m	0,027 m

Tab. 32: Results of statistical evaluation

The statistical parameters were:

- standard deviation s_1 = 0,244
- variance 24,4%
- number of results n = 135
- k-factor k_n = 1,68

The value of the spring stiffness for mineral wool is approximately 50% to 70% of the value for the foamed core materials PUR and EPS. This is a better ratio than for c_1 which might result from the reduction of the negative effects of the lower shear stiffness when the fastener is acting as a point load. The influence of the stiffness of the faces was investigated, too: From the statistical evaluation an additional reduction factor of c_F = 0,46 for faces made of GFRP was obtained, so the value c_F = 0,43 determined above should be used. The thickness of GFRP faces has to be in the range of 1,70 mm to 2,00 mm. No reduction factor for aluminium faces is required.

Finally we obtain

$$c_{\vartheta 2,mean} = c_{2,mean} \cdot c_F \cdot n \cdot b_K^2 \cdot E_C \qquad \textbf{(33)}$$

and

$$c_{\vartheta 2,k} = c_{2,k} \cdot c_F \cdot n \cdot b_K^2 \cdot E_C \qquad \textbf{(34)}$$

Due to the different mechanical model, the numerical parameters deviate from the ones given in [3] by order of approximately 10.

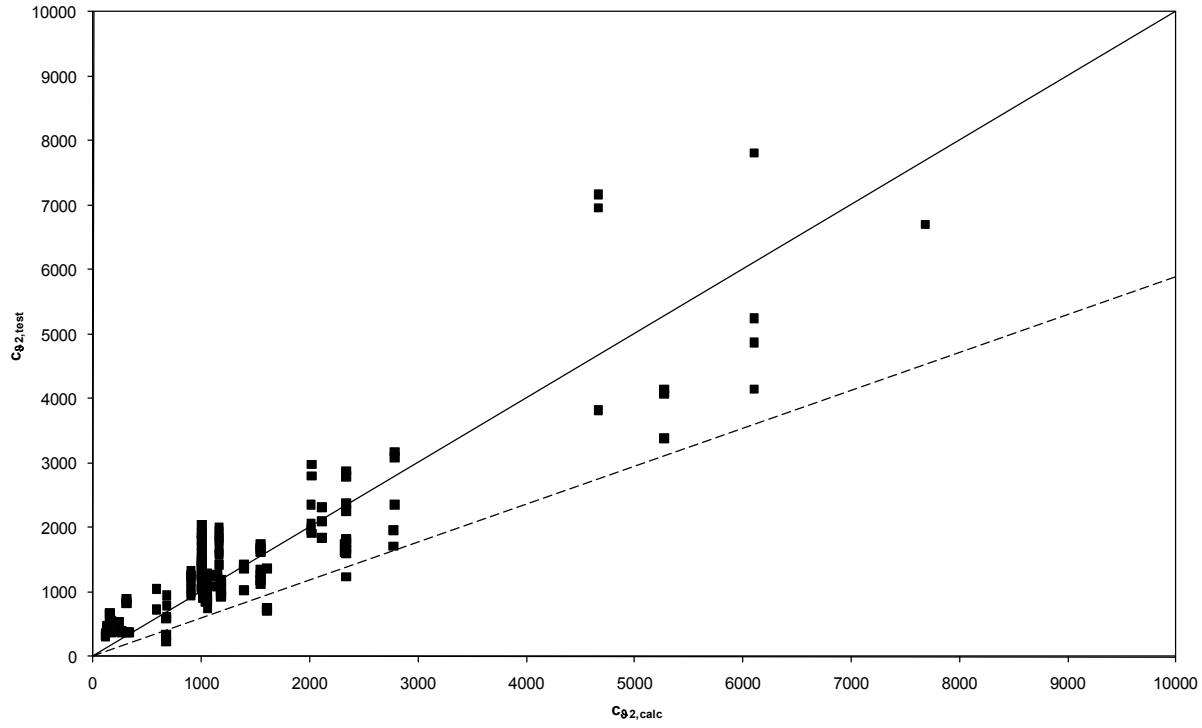

Fig. 40: Comparison of tests results with calculated values for foamed core material

6.4 Creep effects

Creep-effects have to be taken into account for panels under long-term loading (such as self-weight or snow). Creep effects lead to an increase of deformations, such reducing the stiffness and therefore the restraint. This will lead to a decrease in the values of $c_{\vartheta 2}$, but will not affect $c_{\vartheta 1}$. Normally this is done by using a time-dependant reduction factor $\varphi_{C,t}$ for the stiffness of the core material.

$$E_{C,t} = \frac{E_C}{1+\varphi_{C,t}} \tag{35}$$

For the determination of this factor we refer to existing test data: During creep bending tests to obtain the increase in deflection because of creep also the indentation of the support into the panel was measured.

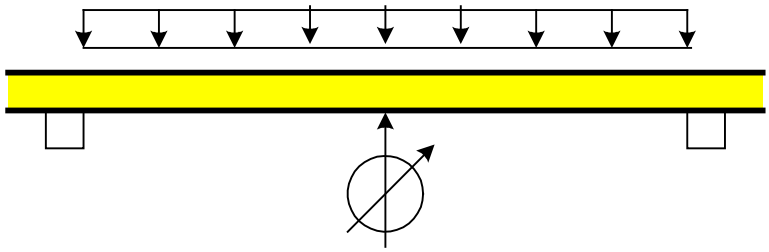

Fig. 41: Test set-up for creep bending tests according to EN 14509

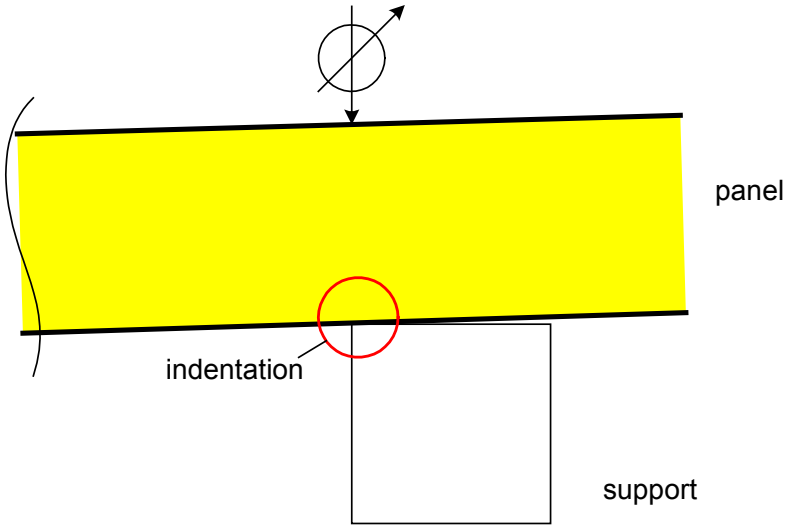

Fig. 42: Measurement of the indentation at the supports during creep bending tests

This data will be used for the derivation of the reduction factor. Fig. 43 and Fig. 44 show the increase in compression by using a normalised indentation

$$\varphi_{C,t} = \frac{\Delta u(t)}{u_0} = \frac{u(t)-u_0}{u_0} \tag{36}$$

both for PUR and mineral wool.

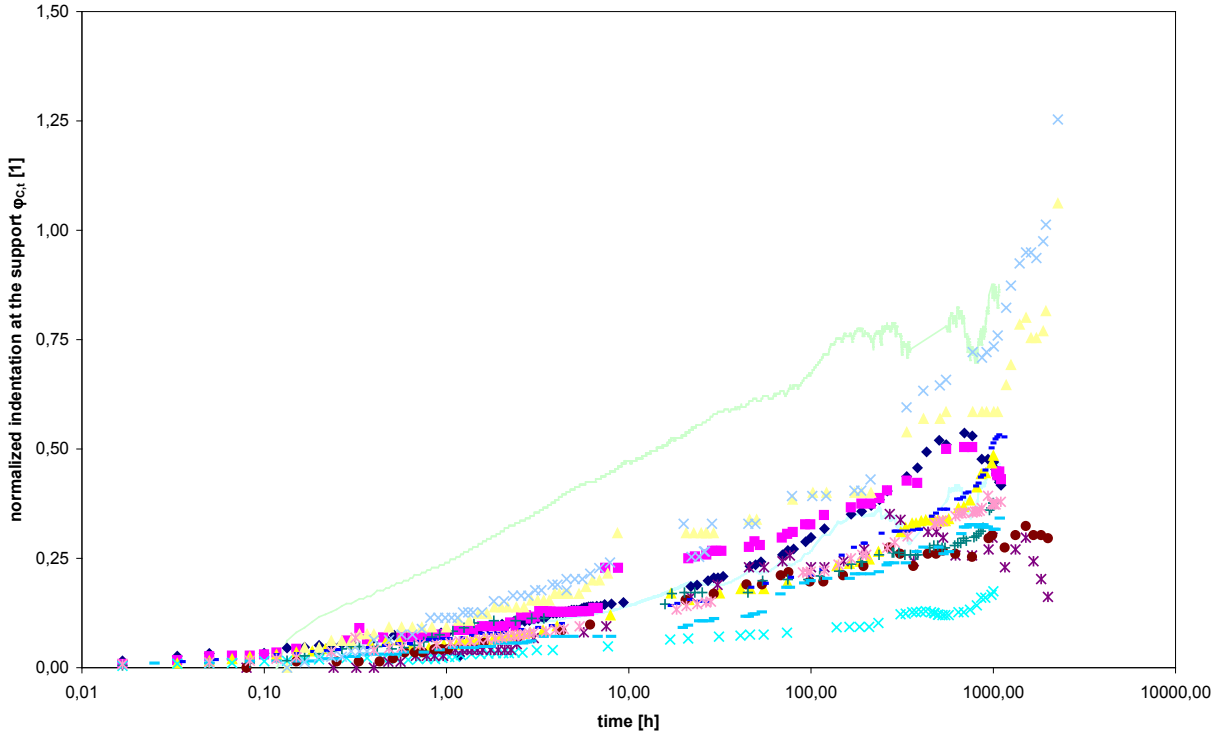

Fig. 43: $\varphi_{c,t}$ for panels with a core made of PUR

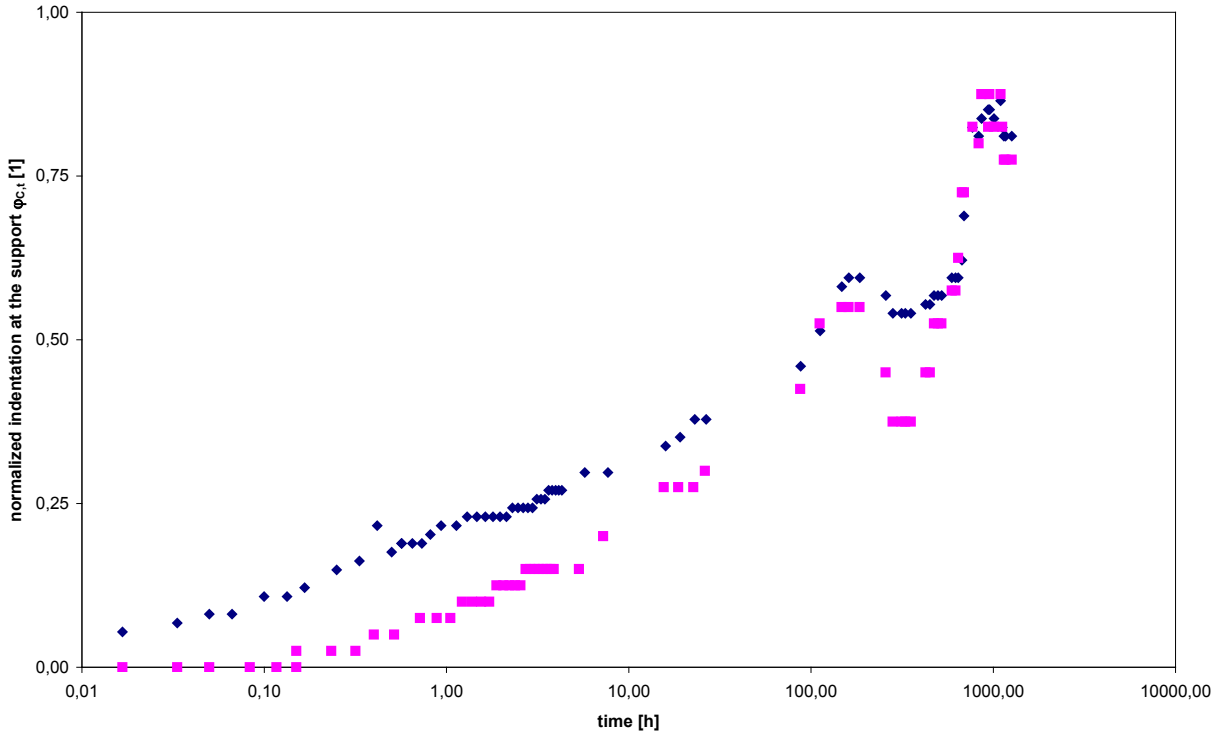

Fig. 44: $\varphi_{c,t}$ for panels with a core made of mineral wool

These tests were evaluated according to EN 14509: The increase in indentation after 200 h and 1000 h were used for an extrapolation to 2000 h (representing snow loading) and 10000 h

(representing self-weight loading). These extrapolated values were checked by comparison with the results of three tests for which data for 2000 h exist.

Test No.	Core material	Measured values			Extrapolated values	
		$\varphi_{C,200}$	$\varphi_{C,1000}$	$\varphi_{C,2000}$	$\varphi_{C,2000}$	$\varphi_{C,10000}$
1	PUR	0,364	0,477	-	0,631	0,800
2		0,375	0,504	-	0,671	0,873
3		0,242	0,484	-	0,706	1,176
4		0,093	0,174	-	0,251	0,406
5		0,278	0,297	-	0,366	0,351
6		0,233	0,303	0,303	0,400	0,503
7		0,242	0,376	-	0,520	0,759
8		0,292	0,520	-	0,742	1,172
9		0,214	0,321	-	0,440	0,627
10		0,349	0,470	-	0,626	0,816
11		0,767	0,855	-	1,071	1,107
12		0,400	0,585	0,859	0,797	1,114
13		0,412	0,732	1,057	1,044	1,647
14		0,134	0,194	-	0,264	0,366
15		0,194	0,281	-	0,382	0,530
16	MW	0,595	0,851	-	1,153	1,583
17		0,550	0,875	-	1,218	1,805

Tab. 33: Creep factors $\varphi_{C,t}$ obtained from tests

A statistical evaluation was done for all values to obtain a 5%-fractile using a log-normal distribution. This was done separately for both core materials.

Core material	$\varphi_{C,2000}$		$\varphi_{C,10000}$	
	mean	characteristic	mean	characteristic
PUR	0,594	1,287	0,816	1,833
MW	1,185	1,349	1,694	2,309

Tab. 34: Statistical evaluation of creep factors $\varphi_{C,t}$

The low number of tests with mineral wool core lead to an increase in the k-value, but also to an decrease a reduction in scatter. Therefore the final values are quite similar for both core materials.

These values will be compared with the results form [3]. In [3], a constant factor for the reduction of the stiffness of ξ_2 = 0,5 is assumed. This factor can be assumed to be valid for long-time self-weight loading and leads to $\varphi_{C,10000}$ = 2,0 which is quite similar to the value obtained

above. To take into account the creep effects, the elastic modulus $E_{C,t}$ of the core material for calculating $c_{\vartheta 1}$ and $c_{\vartheta 2}$ should be used. This value can be calculated by

$$E_{C,t} = \frac{E_C}{1+\varphi_{C,t}} \quad \textbf{(37)}$$

with the characteristic values of Tab. 35.

Core material	$\varphi_{C,2000}$	$\varphi_{C,10000}$
PUR	1,287	1,833
MW	1,349	2,309

Tab. 35: Creep factors $\varphi_{C,t}$

7 Summary

Because of their high bending stiffness sandwich panels can be used to stabilise beams against lateral torsional buckling. In report D3.3 – part 1 the evaluation of tests for the determination of the stiffness of the connection between beams and panels is given. A summary is given in the appendix which also includes information on the application range.

8 References

[1] Katnam, K.B.; Van Impe, R., Lagae, G.; De Strycker, M.: Modellimg of cold-formed steel sandwich purlin-sheeting systems too estimate the torsional restraint. Thin-walled structures 45 (2007), p. 584-590.

[2] Schueremans, L.: Rotational restraint by profiled sheeting – an extensive set of Peköz tests validating existing numerical models. Proceedings of EUROSTEEL 2008, p. 87-92.

[3] Dürr, M. 2008. Die Stabilisierung biegedrillknickgefährdeter Träger durch Sandwichelemente und Trapezbleche. Karlsruhe: Berichte der Versuchsanstalt für Stahl, Holz und Steine der Universität Fridericiana in Karlsruhe, 5. Folge Heft 17.

[4] Misiek, Th., Käpplein, S., Dürr, M., Saal, H.: Stabilisation of purlins by sandwich panels – new regulations and recent research results. CIB World Congress 2010. Proceedings.

[5] Lindner, J., Gregul, T.: Drehbettungswerte für Dacheindeckungen mit unterlegter Wärmedämmung. Stahlbau 58 (1989), p. 173-179.

[6] Gehring, A.: Beurteilung der Eignung von metallischem Band und Blech zum Walzprofilieren. Karlsruhe: Berichte der Versuchsanstalt für Stahl, Holz und Steine der Universität Fridericiana in Karlsruhe, 5. Folge Heft 19.

[7] Preliminary European Recommendations for the Testing and Design of Fastenings for Sandwich Panels: ECCS - European Convention for constructional steelwork, TWG 7.9 Sandwich panels and related structures & CIB - International Council for Research and Innovation in Building Construction, W056 Lightweight Constructions. Brussels/Rotterdam 2009.

[N1] DIN 18800-2:2008-11: Stahlbauten – Teil 2: Stabilitätsfälle – Knicken von Stäben und Stabwerken (Steel structures - Part 2: Stability - Buckling of bars and skeletal structures)

[N2] EN 1933-1-3:2006: Eurocode 3: Design of steel structures - Part 1-3: General rules - Supplementary rules for cold-formed members and sheeting

[N3] EN 14509:2006: Self-supporting double skin metal faced insulating panels - Factory made products - Specifications

Summary:

The torsional restraint by sandwich panels can be calculated by using the mechanical model of a torsion spring with the spring stiffness $c_{\vartheta,k}$.

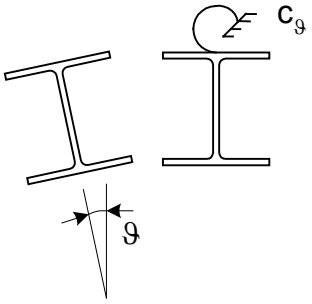

Figure 1: Stabilisation: torsional restraint

This spring stiffness is a combination of the bending stiffness of the attached panel $c_{\vartheta C}$, the stiffness of the connection $c_{\vartheta A}$ and the distortional stiffness $c_{\vartheta B}$ of the beam to be stabilized. The stiffnesses $c_{\vartheta C,k}$ and $c_{\vartheta B,k}$ depend on the geometry of the sandwich panels and type of beams used, see EN 1993-1-1 and EN 1993-1-3. The calculation of $c_{\vartheta A}$ is explained here. In the following text, the stiffness $c_{\vartheta A}$ will be simply denoted as c_ϑ to ease reading and to reduce the number of subscripts.

Figure 2 shows a typical moment-rotation-relation and its generalized form for design for the spring stiffness of the connection of a sandwich panel under downward loading.

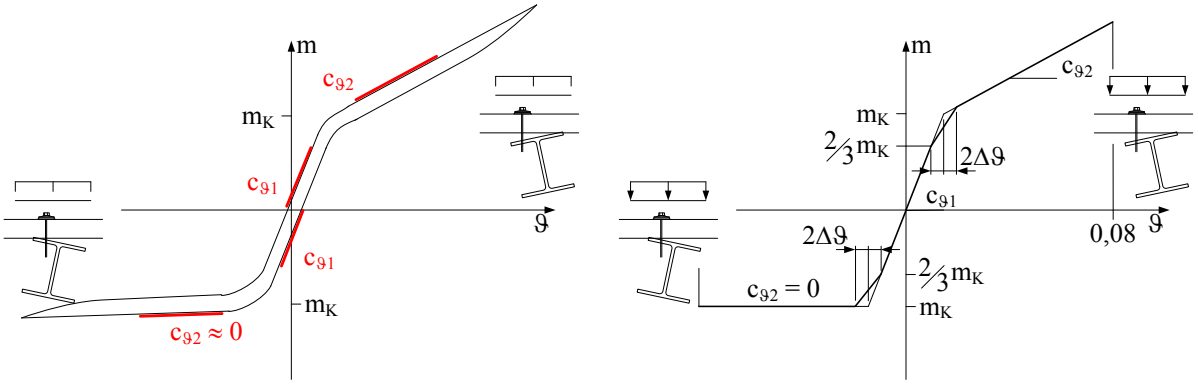

Figure 2: Typical moment-rotation-relation and generalized design moment-rotation-relation

For uplift loading, no torsional restraint is given. Using the simplified moment-rotation relation shown in Figure 2, a secant value (Figure 3) of

$$c_\vartheta = \frac{m_K}{\vartheta(m_K)}$$

can be taken into account for downward loading.

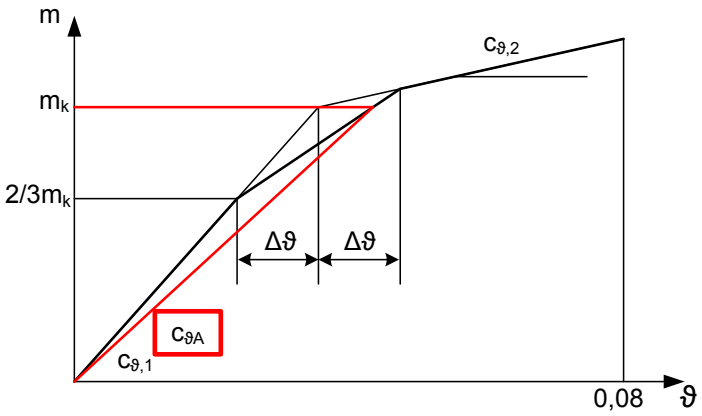

Figure 3: Definition of c_ϑ

The necessary values and parameters are given in the following tables.

	Double-symmetric beams	Z- or C-section
$c_{\vartheta 1}$	$c_1 \cdot c_F \cdot E_{C,t,\theta} \cdot b^2$	$c_1 \cdot c_F \cdot E_{C,t,\theta} \cdot b^2$
$c_{\vartheta 2}$	$c_2 \cdot c_F \cdot n \cdot E_{C,t,\theta} \cdot b_K^2$	0
$E_{C,t,\theta}$	$E_{C,t,\theta} = \frac{E_C}{1+\varphi_{C,t}} \cdot \sqrt{k_1^3} = \frac{E_C}{1+\varphi_{C,t}} \cdot \frac{E_{Ct,+80°C}}{E_{Ct,+20°C}}$	
m_K	$q_d \cdot \frac{b}{2}$	$q_d \cdot b$

Table 1: Values $c_{\vartheta 1}$ and $c_{\vartheta 2}$

c_1, c_2	Parameters according to Table 3
c_F	parameter depending on the face material c_F = 1.00 face materials steel and aluminium c_F = 0.38 face material GFRP
$\varphi_{C,t}$	parameter depending on the duration of loading $\varphi_{C,2000}$ =1,29 core materials PUR and EPS $\varphi_{C,100000}$ =1,83 core materials PUR and EPS $\varphi_{C,2000}$ =1,35 core material mineral wool $\varphi_{C,100000}$ =2,31 core material mineral wool
b [mm]	width of the flange of the beam
b_K [mm]	distance between governing line of fixing and contact line, see Figure 4.
n [m^{-1}]	number of fasteners per meter length in the governing line of fixing (n = 0,0 for hidden fixings and for b_K < 0.5 b)
q_d	design value of the downward load to be transferred from the panel to the beam

Table 2: Parameters

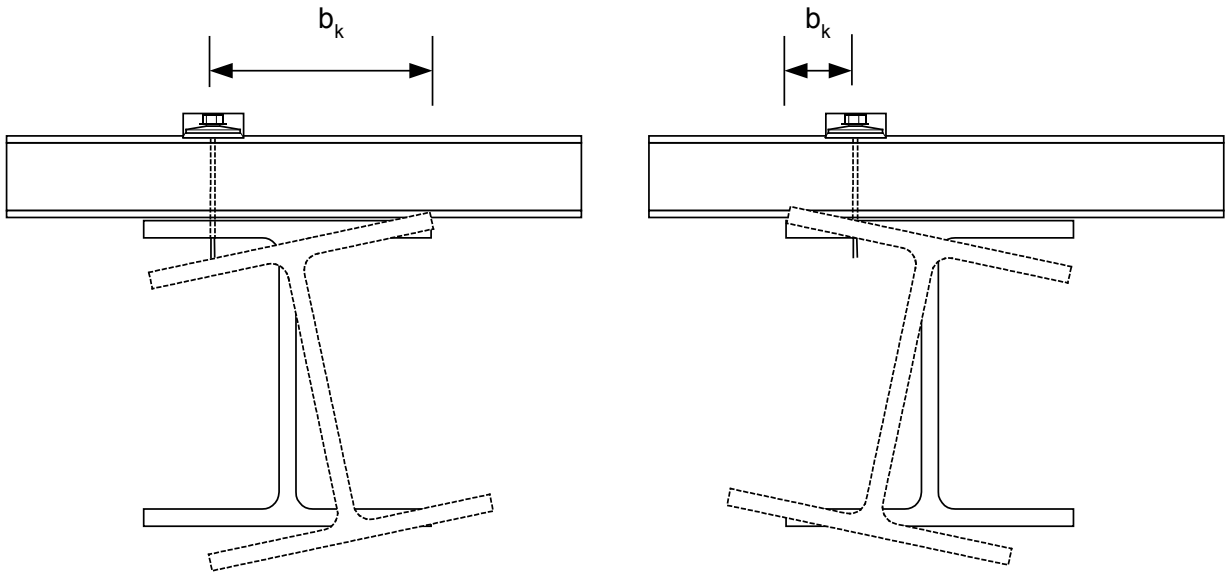

Figure 4: Definition of b_K

Core material	geometry of outer face (at the head of fasteners)	c_1	c_2
PUR/EPS	profiled	0,180	0,052 m
	lightly profiled/flat	0,142	0,040 m
Mineral wool	profiled	0,089	0,027 m
	lightly profiled/flat	0,048	0,027 m

Table 3: Parameters c_1 and c_2

The application range has to be taken into account, see Table 4. If higher values of parameters occur, the calculation procedure is applicable, but the values should be reduced to the upper limits of the application range. It is assumed that the sandwich panels fulfil the basic requirements of EN 14509.

60 mm ≤ b ≤ 180 mm	for double-symmetric beams
60 mm ≤ b ≤ 80 mm	for Z- or C-sections
2,0 N/mm² ≤ E_C ≤ 8,0 N/mm²	Young's modulus of the core material
0,38 mm ≤ t_K ≤ 0,71 mm	sheet thickness of the face layers (steel)
0,50 mm ≤ t ≤ 0,65 mm	sheet thickness of the face layers (aluminium)
1,7 mm ≤ t ≤ 2,0 mm	sheet thickness of the face layers (GFRP)
1 m^{-1} ≤ n ≤ 4 m^{-1}	number of fasteners per meter length in the governing line of fixing
q_d	torsional restraint is only provided with downward loading and only for predominantly static loading
d_W ≥ 16 mm	diameter of washer
ϑ ≤ 0,08 rad	rotation

Table 4: Application range